POLITECNICO DI MILANO





Identification and control of multirotor UAVs

Marco Lovera

Aerospace Systems and Control Laboratory
Department of Aerospace Science and Technology

Outline

- Introduction and motivations
- Modelling and identification
- Robust attitude control
- Control design procedure test case
- Concluding remarks

Introduction

The interest in multirotors as platforms for both research and commercial Unmanned Aerial Vehicle (UAV) applications is steadily increasing:

- ✓ surveillance & security
- ✓ environment monitoring & remote sensing
- ✓ building & industrial plants monitoring
- ✓ photogrammetry

Advantages w.r.t. classical helicopter architecture:

- ✓ simpler rotor articulation (no swash plate, no cyclic command)
- ✓ weak DoFs coupling → easier to control
- ✓ possibility of rotors protection (shrouding) → safer

Possible quadrotor architectures:

- variable RPM (fixed blade pitch) → simple and light rotors hub
- variable pitch (fixed RPM) → avoid performance limitation due to bandwidth of motors dynamics

Some of the envisaged applications lead to tight performance requirements on the attitude control system → this calls for increasingly accurate dynamics models of the vehicle's response to which advanced controller synthesis approaches can be applied

Motivations

Development of an integrated, highly automated, control design tool-chain aimed at fast and reliable deployment of vehicle's attitude control system

Identification experiments indoor on proper test-bed, avoiding risky and time consuming in-flight test campaign

→ Identification of LTI attitude response models

→ Attitude controller tuning solving structured H_∞ robust design problem

→ GOAL: demonstrate that it guarantees acceptable performance also in flight near hover conditions

ANTEOS P2-A2 prototype

- ✓ Variable collective pitch (fixed RPM)
- ✓ MTOW = 5 kg
- ✓ Rotors radius = 0.27 m
- ✓ Arms length = 0.415 m

Quadrotor control: basic principles

h → hovering (fixed point flight)

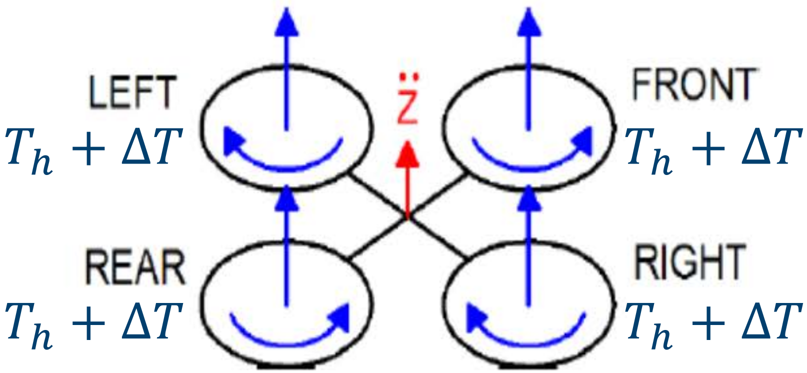

Vertical

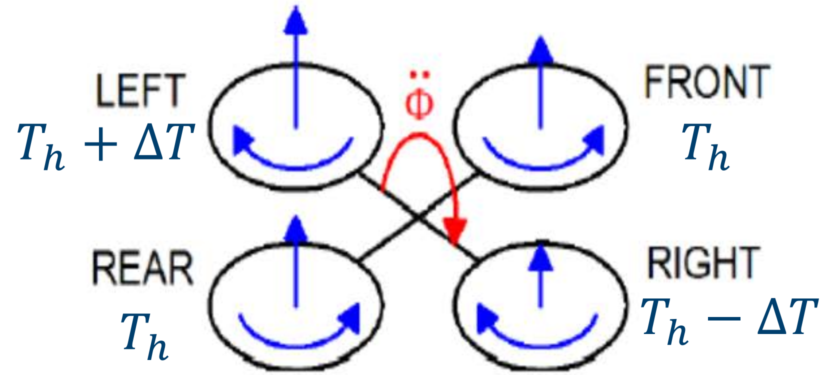

Roll → Lateral

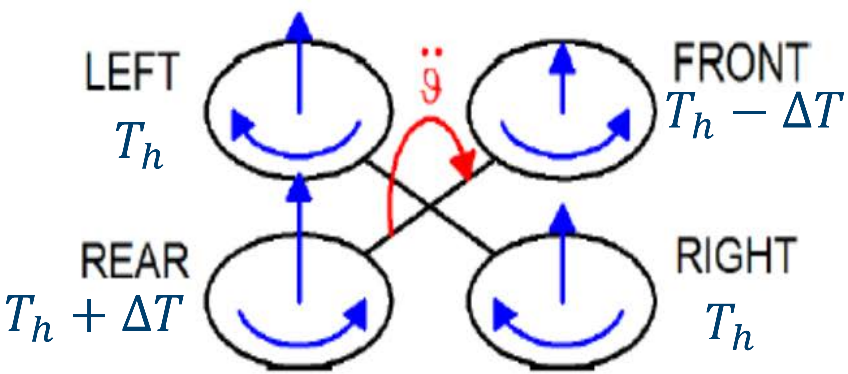

Pitch → Longitudinal

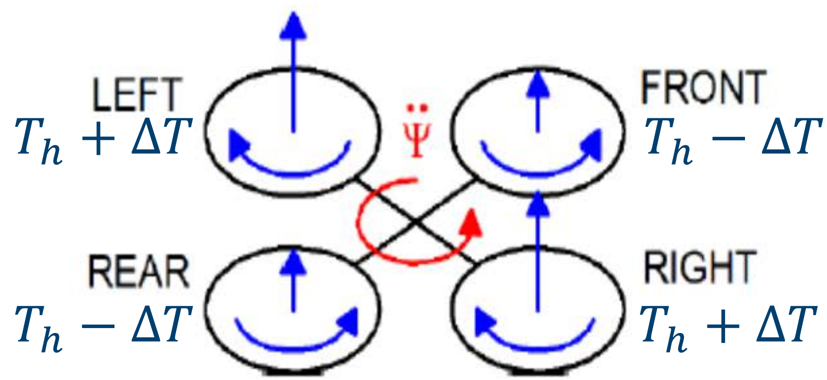

Yaw

Underactuated with respect to 6 DoFs

Quadrotor modeling: reference frame

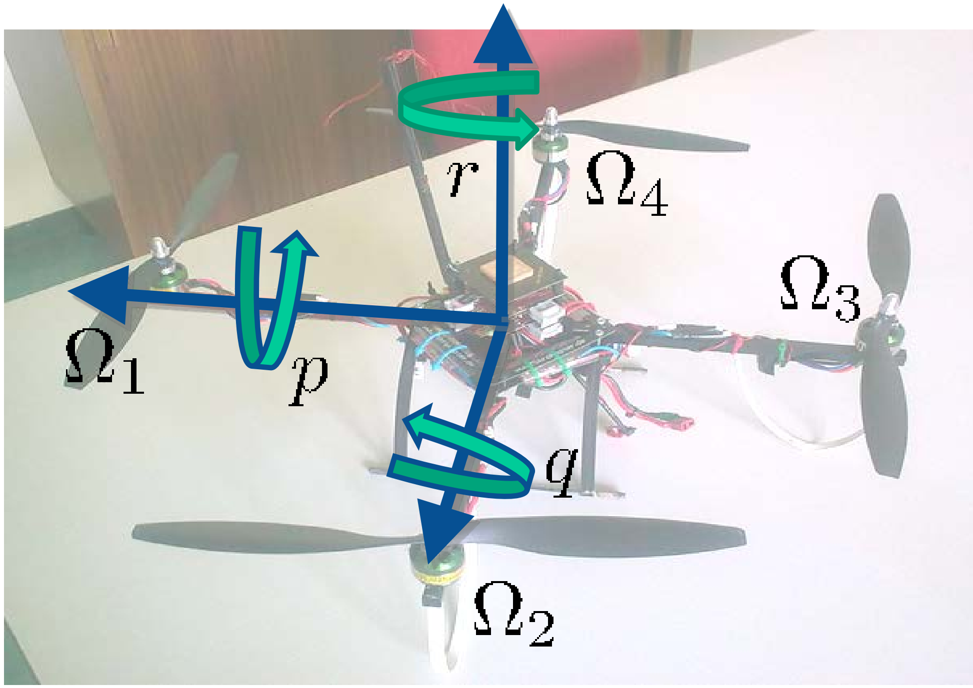

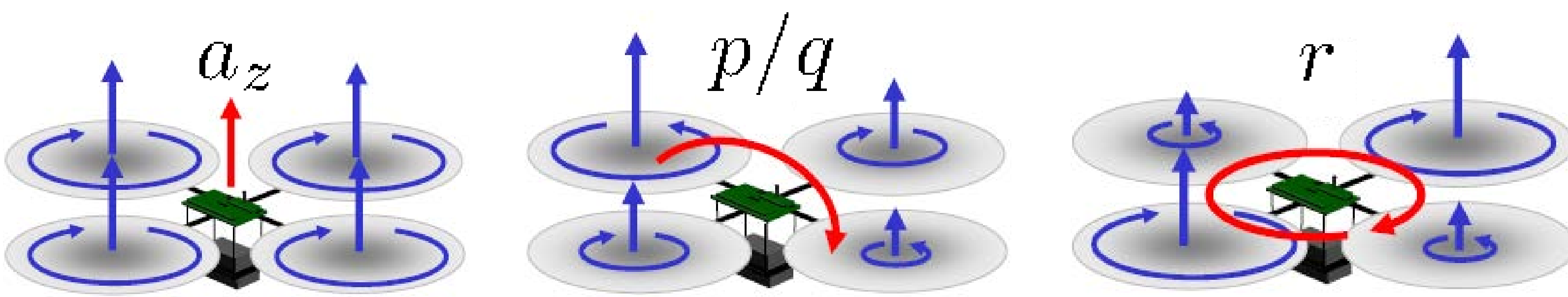

- Collective (U_{col})
- Pitch/Roll (U_{lon}/U_{lat})
- Yaw (U_{ped})

Elementary aerodynamic model:

the thrust generated by each rotor is proportional to Ω^2:

$$F_i = b\Omega_i^2, \quad i = 1, \ldots, 4$$

therefore the total thrust is given by

$$F = \sum_{i=1}^{4} F_i = b\sum_{i=1}^{4} \Omega_i^2$$

while the rolling/pitching moments are given by

$$M_p = l(F_4 - F_2) = l(\Omega_4^2 - \Omega_2^2)$$

$$M_q = l(F_3 - F_1) = lb(\Omega_3^2 - \Omega_1^2)$$

and the yawing moment is

$$M_r = F_2 + F_4 - F_1 - F_3 = d(\Omega_2^2 + \Omega_4^2 - \Omega_1^2 - \Omega_3^2)$$

Control variables

The control variables are commonly defined as:

- Collective
$$U_{col} = \Omega_1^2 + \Omega_2^2 + \Omega_3^2 + \Omega_4^2$$
- Roll
$$U_{lat} = \Omega_4^2 - \Omega_2^2$$
- Pitch $U_{lon} = \Omega_3^2 - \Omega_1^2$
- Yaw $U_{ped} = \Omega_2^2 + \Omega_4^2 - \Omega_1^2 - \Omega_3^2$

with respect to which

- Collective $F = bU_{col}$
- Roll $M_p = blU_{lat}$
- Pitch $M_q = blU_{lon}$
- Yaw $M_r = dU_{ped}$

Overall model which describes the behavior of a quadrotor helicopter

$$m\,\dot{V}_b + \omega_b \times (mV_b) = F_g + F_{props}$$
$$I_n\,\dot{\omega}_b + \omega_b \times (I_n\omega_b) = M_{damp} + M_{props}$$

Gravity component

$$F_g = T_{BE}(\Phi,\Theta,\Psi)\begin{bmatrix} 0 \\ 0 \\ mg \end{bmatrix} = \begin{bmatrix} -S_\Theta \\ S_\Phi C_\Theta \\ C_\Phi C_\Theta \end{bmatrix} mg.$$

Damping component

$$M_{damp} = \begin{bmatrix} \frac{\partial L}{\partial p} & 0 & 0 \\ 0 & \frac{\partial M}{\partial q} & 0 \\ 0 & 0 & \frac{\partial N}{\partial r} \end{bmatrix}\begin{bmatrix} p \\ q \\ r \end{bmatrix}$$

$$F_{props} = -\begin{bmatrix} 0 \\ 0 \\ K_T\left(\Omega_1^2 + \Omega_2^2 + \Omega_3^2 + \Omega_4^2\right) \end{bmatrix}$$

$$M_{props} = \begin{bmatrix} K_T\frac{b}{\sqrt{2}}\left(\Omega_1^2 - \Omega_2^2 - \Omega_3^2 + \Omega_4^2\right) \\ K_T\frac{b}{\sqrt{2}}\left(\Omega_1^2 + \Omega_2^2 - \Omega_3^2 - \Omega_4^2\right) \\ K_Q\left(-\Omega_1^2 + \Omega_2^2 - \Omega_3^2 + \Omega_4^2\right) \end{bmatrix}$$

Dynamics of a quadrotor helicopter

$$\dot{\phi} = p + \sin(\phi)\tan(\theta)\, q + \cos(\phi)\tan(\theta)\, r$$

$$\dot{\theta} = \cos(\phi)\, q - \sin(\phi)\, r$$

$$\dot{\psi} = \frac{\sin(\phi)}{\cos(\theta)}\, q + \frac{\cos(\phi)}{\cos(\theta)}\, r$$

$$\ddot{z} = -g + (\cos(\theta)\ \cos(\phi))\, \frac{1}{m}\, F$$

$$\dot{p} = \frac{I_y - I_z}{I_x}\, q\, r + \frac{1}{I_x}\, M_p$$

$$\dot{q} = \frac{I_z - I_x}{I_y}\, p\, r + \frac{1}{I_y}\, M_q$$

$$\dot{r} = \frac{I_x - I_y}{I_z}\, p\, q + \frac{1}{I_z}\, M_r$$

Accelerometer and magnetometer

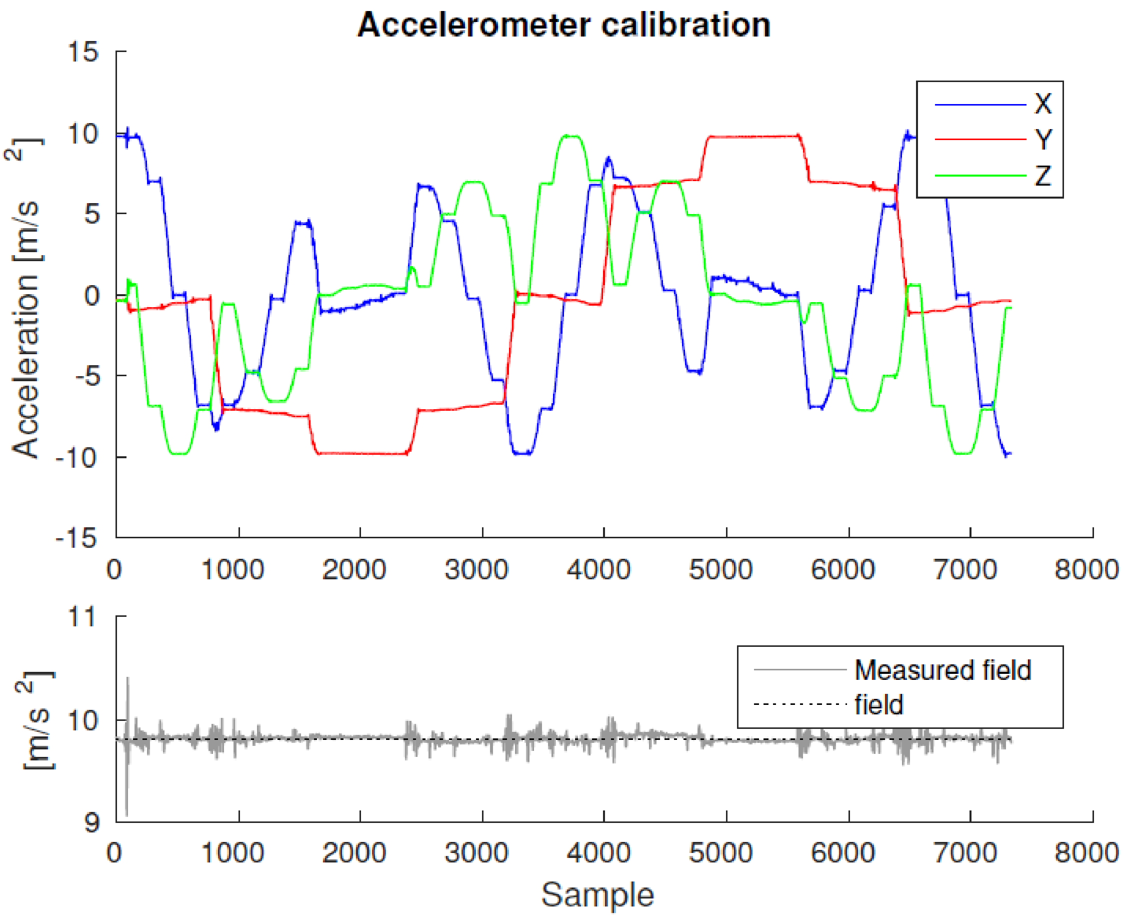

Gyroscope

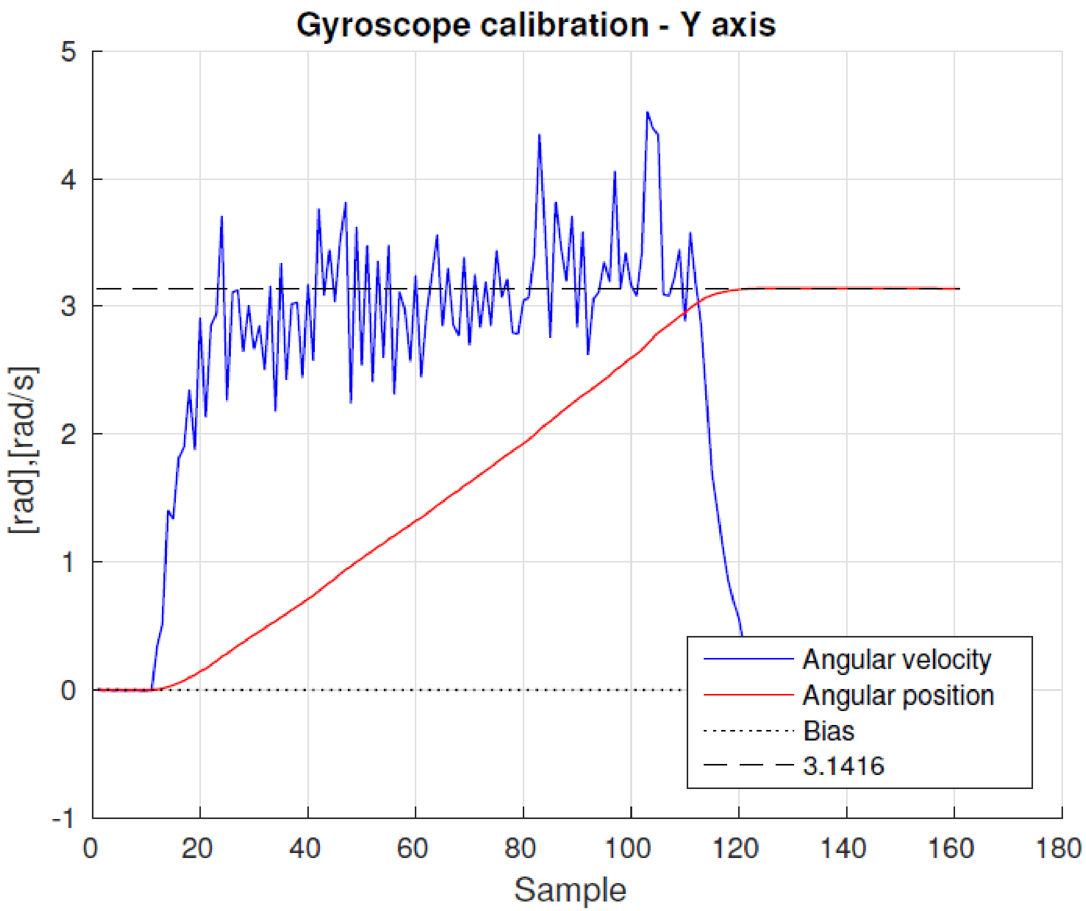
Gyroscope calibration - Y axis
[rad],[rad/s]
Sample
5
4
3
2
1
0
-1
0
20
40
60
80
100
120
140
160
180
Angular velocity
Angular position
Bias
3.1416

TESTING PLATFORM

To measure the propeller's thrust against the rotational speed

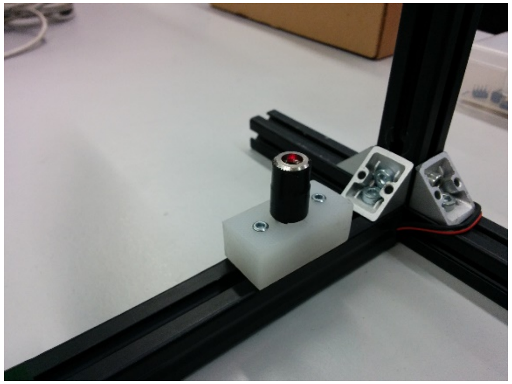

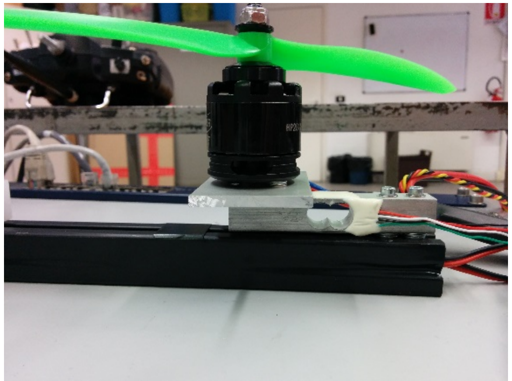
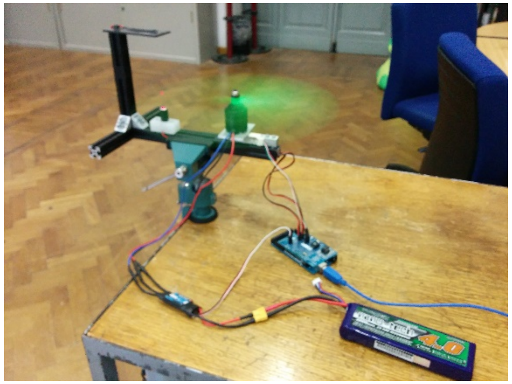

- Sensors
  - Load cell
    -> Thrust
  - Optical tachometer
    -> Rotational speed
- Electronic board
  - Arduino MEGA

STATIC RESPONSE ESTIMATION

Relationship between propeller's thrust and rotational speed

$$\widehat{C}_T = \frac{\widehat{K}_T}{\rho A R^2}$$

$$T = K_T \Omega^2$$

$$K_T = C_T \rho A R^2$$

$$\longrightarrow$$

$$\widehat{C}_P = \frac{\widehat{C}_T^{3/2}}{\sqrt{2}}$$

$$\widehat{C}_Q = \widehat{C}_P$$

Relationship between the p $\Omega = \widehat{m} Th_{\%} + \widehat{q}$ rottle and propeller's rotational speed

Actuator analysis

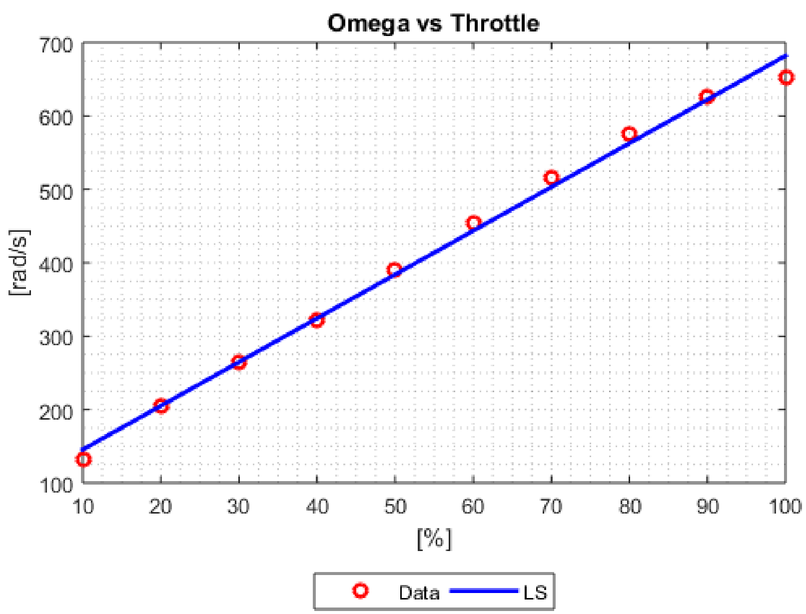

Linear characteristic

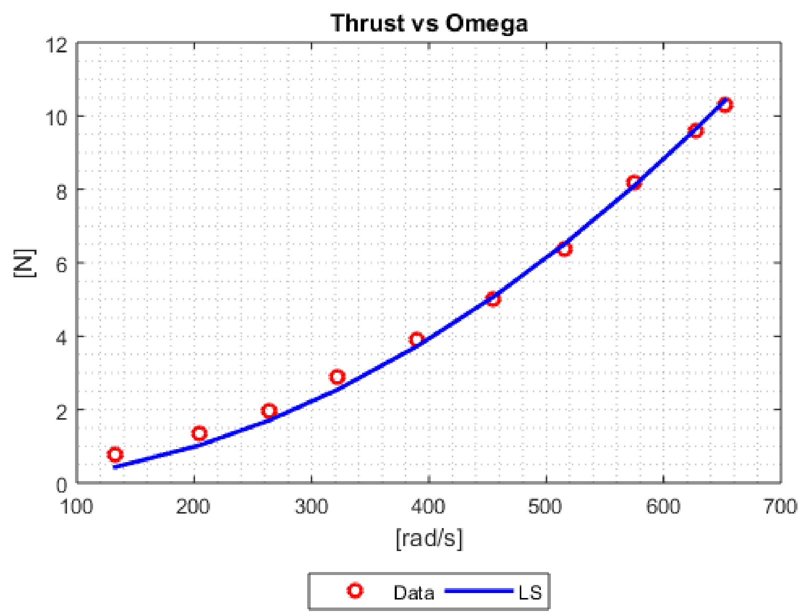

Quadratic characteristic

DINAMIC RESPONSE ESTIMATION

- Assuming a first order dynamical relationship between the percentage of throttle as input and the rotational speed of the propeller as output

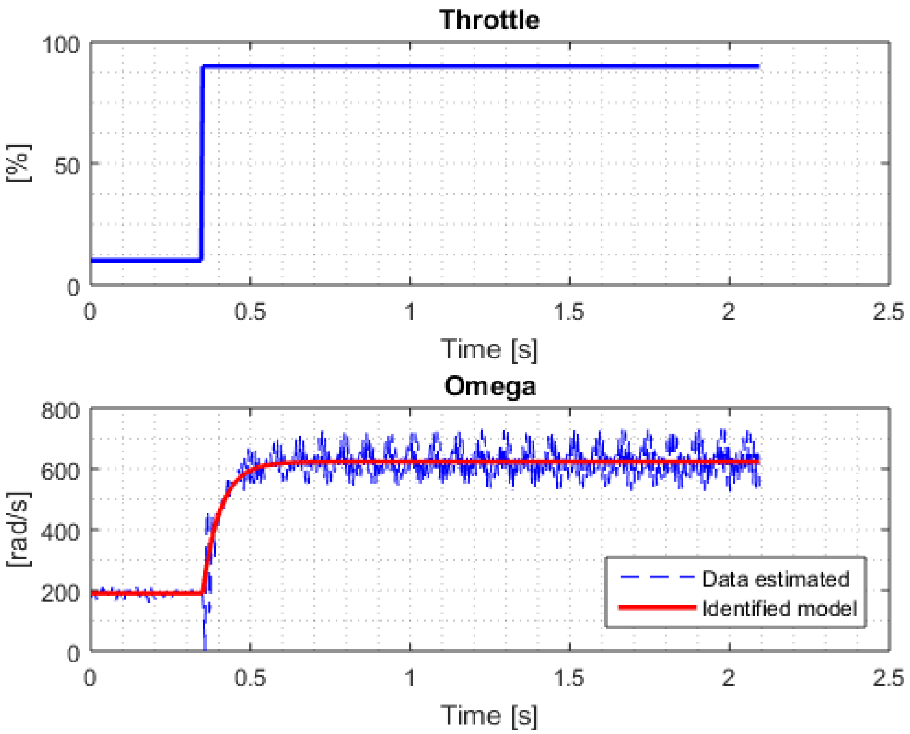

$$G(s) = \frac{\Omega(s)}{Th(s)} = \frac{\widehat{\mu}}{1 + s\widehat{\tau}}$$

- Introduction and motivations
- **Modelling and identification**
- Robust attitude control
- Control design procedure test case
- Concluding remarks

Attitude dynamics identification
State of the art

- It is apparent from literature that quadrotor mathematical models are easy to establish as far the kinematics and dynamics of linear and angular rigid body motion are concerned

- Characterizing aerodynamic effects and additional dynamics such as, *e.g.*, due to actuators and sensors, is far from trivial → increasing interest in experimental characterization of quadrotor dynamics response through system identification

- System identification is actually a well established approach for the development of control-oriented LTI models in the rotorcraft field:
  - ✓ Frequency-domain approaches (*e.g.* NASA CIFER tool)
  - ✓ Iterative time-domain approaches (*e.g.* OE, EE, etc.)
  - ✓ NON-iterative time-domain approaches (*e.g.* subspace methods)

- The application to full scale rotorcraft is fairly mature but less experience has been gathered on small-scale vehicles

- The identification experiments have been carried out in laboratory conditions, using a test-bed that constrains all DoFs except pitch rotation (rotors in OGE)

- Similar experiments have been carried out in flight to ensure that indoor set-up is representative of actual attitude dynamics in near hovering

- Pseudo Random Binary Sequences (PRBS) were selected as excitation signal

- Experiments have been carried out in quasi open-loop conditions:
  - nominal attitude and position controllers were disabled
  - a supervision task enforcing attitude limits (±20°) was left active (inherently fast instability)

Input signal (collective pitch difference between opposite rotor) in identification test

PRBS excitation + feedback action of supervision task , quasi open-loop

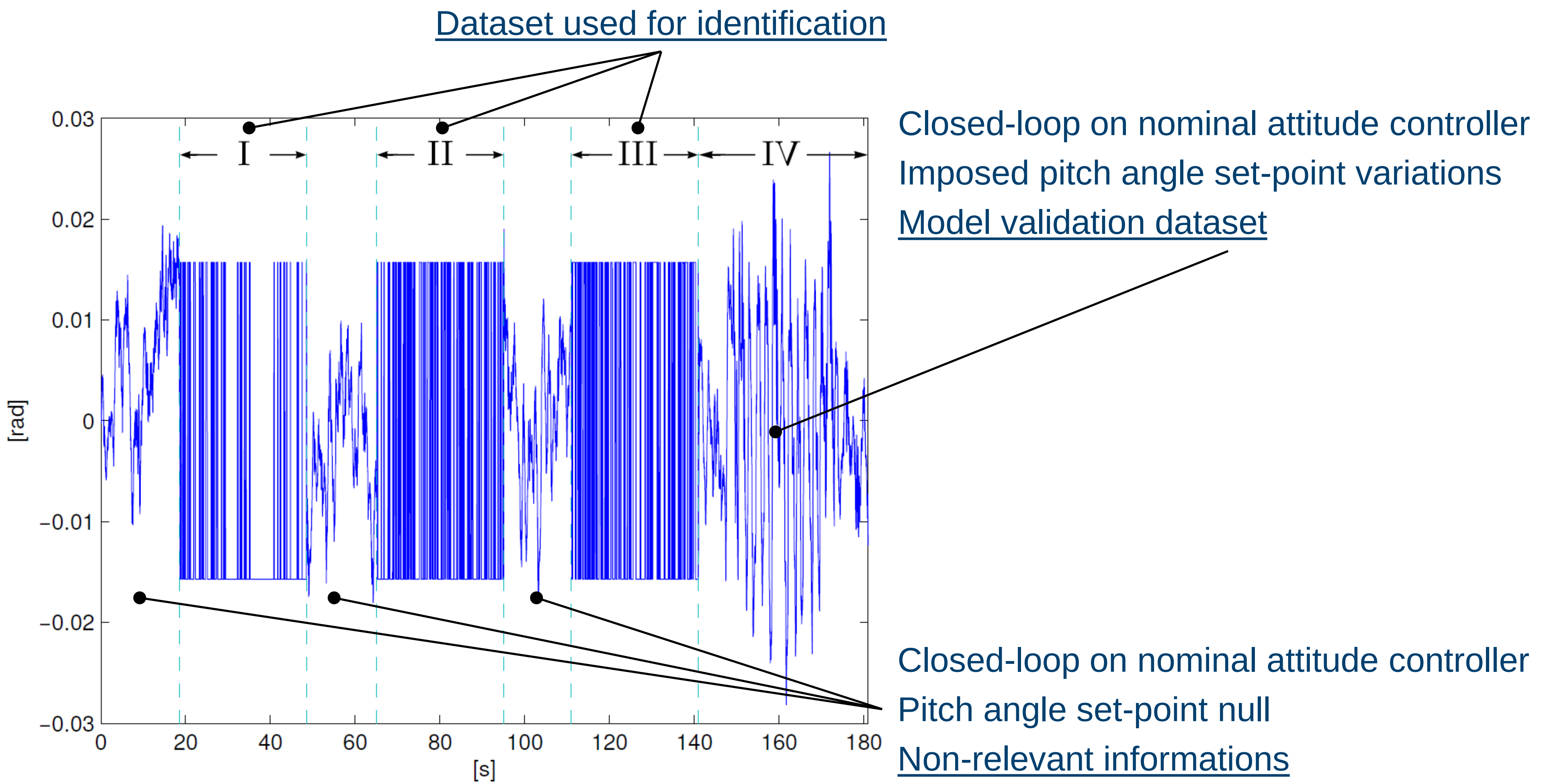

Attitude dynamics identification:
Identification experiments (3)

The parameters of the PRBS (signal amplitude and min/max switching interval) were tuned to obtain:

- ✓ an excitation spectrum consistent with the expected dominant attitude dynamics (4 to 8 rad/s)
- ✓ a reduced second harmonic amplitude

Identification campaign	PRBS switching time range [s]
1	0.05 – 0.1
2	0.1 – 0.2
3	0.2 – 0.4
4	0.4 – 0.8

PRBS amplitude	Blade pitch difference between opposite rotor angle [rad] / command [%]
1	± 0.012 / ± 7
2	± 0.015 / ± 9
3	± 0.019 / ± 11

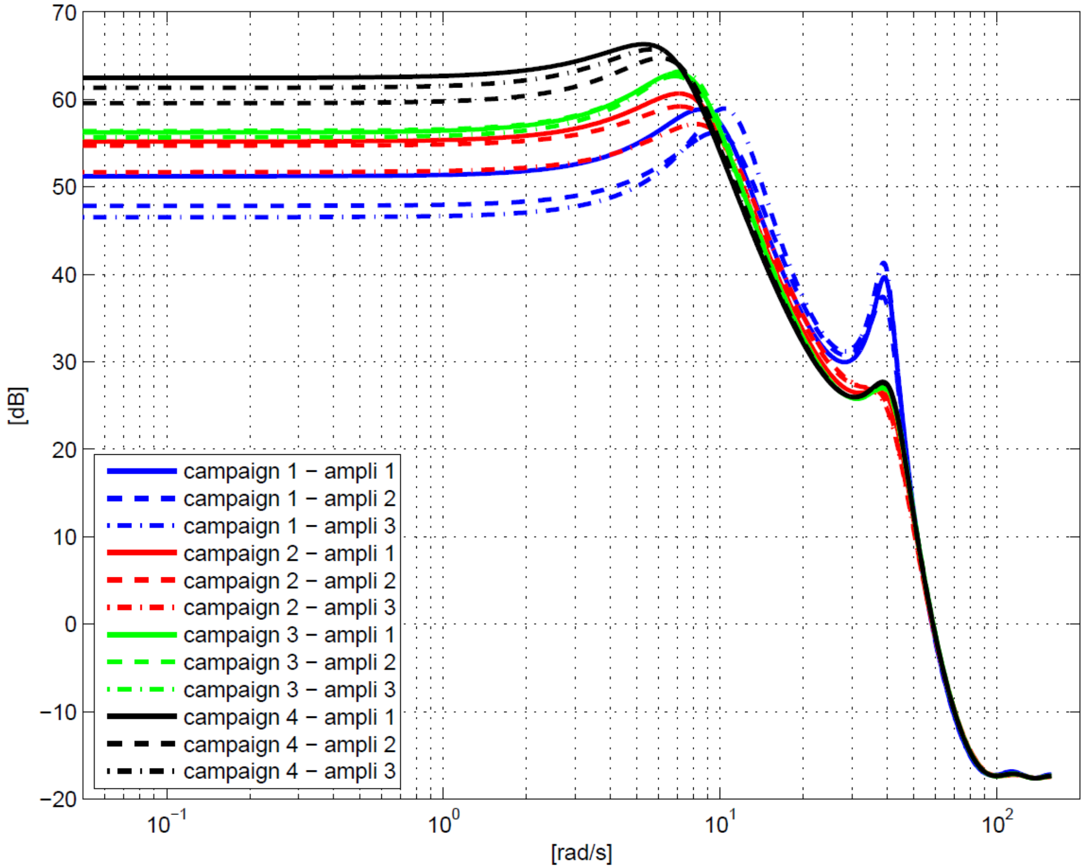

Identification input signal obtained concatenating 3 excitation segments from different test in order to average out mild non-linearities

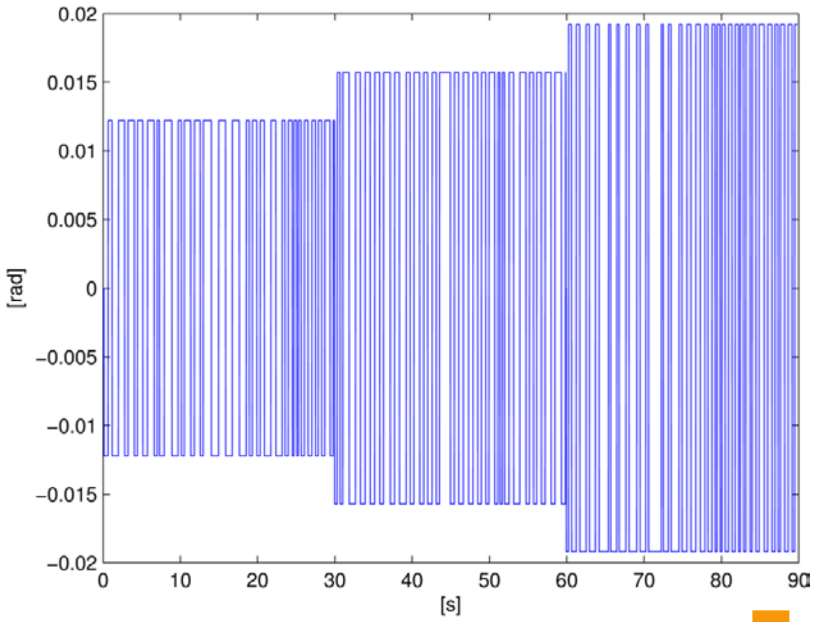

Estimate quality degradation caused by data concatenation is negligible due to large duration of PRBS and small n° of concatenations

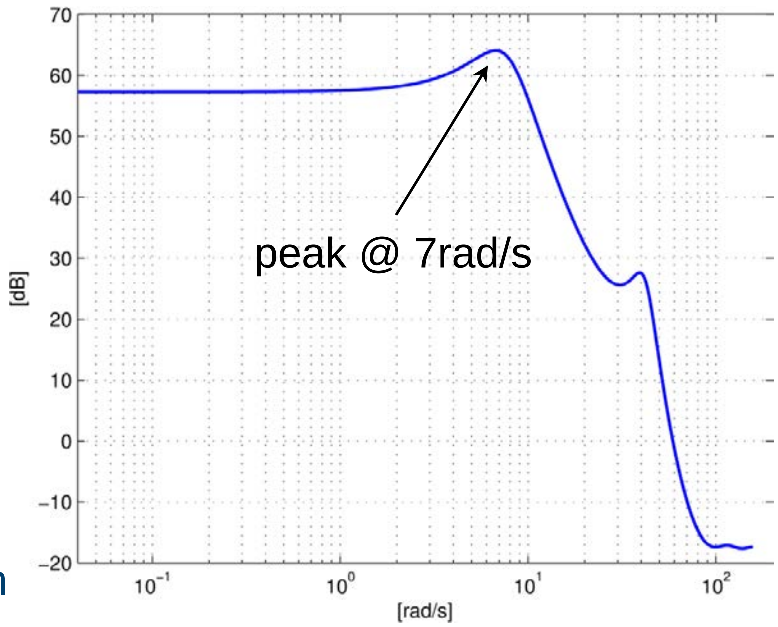

Excitation spectrum

Data logged during test @ 50Hz

Input: pitch attitude control variable

Output: $\theta, q, \dot{q}$ from on-board IMU

BLACK-BOX METHODS: gives unstructured model, non-physically motivated state space

- Subspace Model Identification (SMI) algorithms, non-iterative (efficient computation):
  - PI-MOESP (Past Inputs - Multivariable Output Error State sPace realization)
  - PBSID (Predictor Based System IDentification)

both providing LTI SISO state space model of the pitch rate response to control input

- On-line implementation of the Least Mean Squares (LMS) algorithm:
  - updates recursively on-board an estimate of the SISO impulse response of pitch angular velocity in the form of Finite Impulse Response (FIR) model
  - state space model for the pitch dynamics recovered via Kung's realization

GREY-BOX METHODS: structure imposed a-priori defining a first-principle model for pitch dynamics

- Output Error (OE) Maximum Likelihood (ML) estimation
- H_∞ approach (model matching problem, non-convex & non-smooth optimization)

both determine the unknown physical parameter of structured LTI model via iterative (time consuming) procedure

SMI was proposed about 25 years ago to handle black-box MIMO problems in a numerically stable and efficient way (numerical linear algebra tools) and has proved extremely successful in a number of industrial applications

PI-MOESP (*Verhaegen & Dewilde,1991*) assumes feeding data gathered in open-loop operations

PBSID (*Chiuso,2007*) is a more advanced and recent algorithm respect to MOESP, suitable for dealing with data generated in closed-loop operations

Remark: time delay in system dynamics (from IMU measurements to servo actuation of rotors collective pitch), equal to $\hat{\tau}$ = 0.06s = 3 samples, leads to a non-minimum phase zero in identified model via SMI → applied forward shift of 3 samples on input signal before model identification and reintroduced as delay in model simulations

Consider the discrete time LTI state space model, with $y_t = \tilde{y}_t + v_t$

$$\begin{aligned} x_{t+1} &= Ax_t + Bu_t \\ \tilde{y}_t &= Cx_t + Du_t \end{aligned}$$

❖ STEP1: estimation of coloumn space of extended observability matrix

$$\Gamma = \left[C^T \ \ (CA)^T \ \ (CA^2)^T \ \ \dots \ \ \left(CA^{i-1}\right)^T\right]^T$$

from measured input-output samples $\{u_t, y_t\}$, through the data equation

$$Y_{t,i,j} = \Gamma X_{t,j} + HU_{t,i,j}$$

relating (block) Hankel matrices constructed from I/O samples

$$Y_{t,i,j} = \begin{bmatrix} y_t & \cdots & y_{t+j-1} \\ \vdots & \ddots & \vdots \\ y_{t+i-1} & \cdots & y_{t+i+j-2} \end{bmatrix} \quad U_{t,i,j} = \begin{bmatrix} u_t & \cdots & u_{t+j-1} \\ \vdots & \ddots & \vdots \\ u_{t+i-1} & \cdots & u_{t+i+j-2} \end{bmatrix}$$

$$X_{t,j} = [x_t \ \ x_{t+1} \ \dots \ x_{t+j-1}]$$

and the block-Toeplitz matrix

$$H = \begin{bmatrix} D & 0 & \dots & 0 \\ CB & D & \dots & 0 \\ CAB & CB & \dots & 0 \\ \vdots & \vdots & \vdots & \vdots \\ CA^{i-2}B & CA^{i-3}B & \dots & D \end{bmatrix}$$

From the data equation the PI-MOESP algorithm considers the RQ factorization

$$\begin{bmatrix} U_{t+1,i,j} \\ U_{t,i,j} \\ Y_{t+1,i,j} \end{bmatrix} = \begin{bmatrix} R_{11} & 0 & 0 \\ R_{21} & R_{22} & 0 \\ R_{31} & R_{32} & R_{33} \end{bmatrix} \begin{bmatrix} Q_1 \\ Q_2 \\ Q_3 \end{bmatrix}$$

and a consistent estimate of the coloumn space of Γ is obtained via SVD of matrix R_{32} under assumption that v_t is Gaussian measurement noise, zero mean, uncorrelated with u_t

- STEP2: from the Γ estimate, matrices A and C of the model can be determined exploiting the invariance of observability subspace
- STEP3: solve a linear least square problem to determine B and D matrices

Consider the finite dimensional LTI state space model, where $\{v(k), w(k)\}$ are ergodic sequences of finite variance, possibly correlated with input u

$$x(k+1) = Ax(k) + Bu(k) + w(k)$$
$$y(k) = Cx(k) + Du(k) + v(k)$$

and pass to innovation form through Kalman gain matrix K

$$x(k+1) = \bar{A}x(k) + \tilde{B}z(k)$$
$$y(k) = Cx(k) + Du(k) + e(k)$$

where $z(k) = [u^T(k) \quad y^T(k)]^T$, $\bar{A} = A - KC$, $\bar{B} = B - KD$, $\tilde{B} = [\bar{B} \quad K]$

- STEP1: Data equations derivation, propagating $p-1$ steps forward the state equation

$$x(k+2) = \bar{A}^2 x(k) + [\bar{A}\tilde{B} \quad \tilde{B}] \begin{bmatrix} z(k) \\ z(k+1) \end{bmatrix}$$
$$\vdots$$
$$x(k+p) = \bar{A}^p x(k) + \mathcal{K}^p Z^{0,p-1} \cong \mathcal{K}^p Z^{0,p-1}$$

where $\mathcal{K}^p = [\bar{A}^{p-1}\tilde{B}_0 \quad \dots \quad \tilde{B}]$ is the system extended controllability matrix and

$$Z^{0,p-1} = \begin{bmatrix} z(k) \\ \vdots \\ z(k+p-1) \end{bmatrix}$$

As a consequence the input-output system behavior is

$$y(k+p) \cong C\mathcal{K}^p Z^{0,p-1} + Du(k+p) + e(k+p)$$
$$\vdots$$
$$y(k+p+f) \cong C\mathcal{K}^p Z^{f,p+f-1} + Du(k+p+f) + e(k+p+f)$$

The data equations in matrix notation are given by

$$X^{p,f} \cong \mathcal{K}^p \bar{Z}^{p,f}$$
$$Y^{p,f} \cong C\mathcal{K}^p \bar{Z}^{p,f} + DU^{p,f} + E^{p,f}$$

- STEP2: considering $p = f$ (called past and future windows length), estimates of matrices $C\mathcal{K}^p$ and D are computed solving the LS problem

$$\min_{C\mathcal{K}^p, D} \|Y^{p,p} - C\mathcal{K}^p \bar{Z}^{p,p} - DU^{p,p}\|_F$$

- <u>STEP3</u>: an estimate of the state sequence $X^{p,p}$ can be obtained computing the SVD

$$\Gamma^p X^{p,p} \cong \Gamma^p \mathcal{K}^p \bar{Z}^{p,p} = U\Sigma V^T$$

where Γ^p is the extended observability matrix, from which an estimate of C can be obtained solving the LS problem

$$\min_C \left\| Y^{p,p} - \widehat{D} U^{p,p} - C \widehat{X}^{p,p} \right\|_F$$

- <u>STEP4</u>: estimation of the innovation data matrix $E^{p,f} = Y^{p,p} - \hat{C}\widehat{X}^{p,p} - \widehat{D}U^{p,p}$ and the entire set of system state space matrices, solving the LS problem

$$\min_{A,B,K} \left\| \widehat{X}^{p+1,p} - A\widehat{X}^{p,p-1} - BU^{p,p-1} - KE^{p,p-1} \right\|_F$$

Black-box methods
LMS algorithm (1)

- Alternative black-box model identification method adopted: on-line implementation of the Least Mean Squares (LMS) algorithm

- Updates recursively on board an estimate of the SISO impulse response of pitch angular velocity in the form of Finite Impulse Response (FIR) model

- State space model for the pitch dynamics recovered from estimated impulse response via suitable realization techniques (Kung's algorithm)

Black-box methods
LMS algorithm (2)

An adaptive digital filter consists of two parts:

- digital filter (coefficients are called weights)
- an adaptive algorithm for adjusting the weights

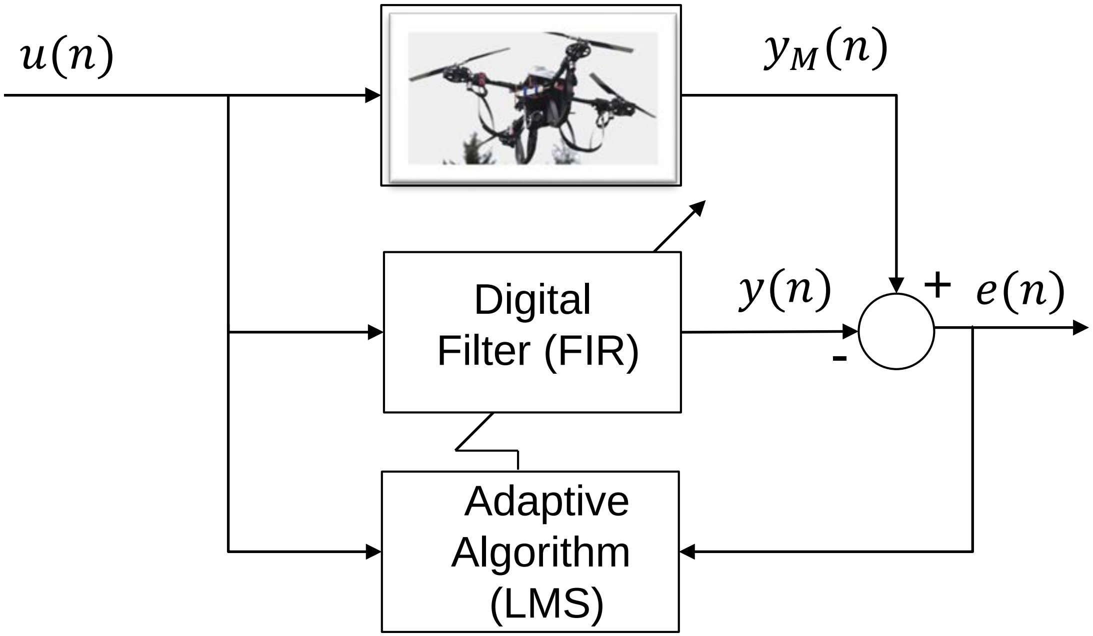

- $u(n)$ input signal
- $y_M(n)$ desired response
- $y(n)$ filter output
- $e(n)$ error

Properties of the FIR filter:

- all the poles are inside the unit cycle (all in the origin): the filter is always stable
- small changes in the weights will give rise to small changes in the filter response

The output of a digital FIR filter is a linear combination of the current and the past input values:

$$y(n) = w_0 u(n) + w_1 u(n-1) + \cdots + w_L u(n-L+1) = \sum_{l=0}^{L-1} w_l u(x - l) = \boldsymbol{w}^T \boldsymbol{u}(n)$$

where

- $\boldsymbol{u}(n) = [u(n) \quad u(n-1) \quad \cdots \quad u(n-L+1)]^T$
- $\boldsymbol{w} = [w_0 \quad w_1 \quad \cdots \quad w_{L-1}]^T$
- L is the length of the filter (number of weights)

The relationship can be represent more easily in the *z*-transform domain using the unit delay operator $z^{-1} \rightarrow z^{-1}u(n) = u(n-1)$:

$$Y(z) = W(z)U(z)$$

where

- $W(z) = \frac{w_0 z^{L-1} + w_1 z^{L-2} + \cdots + w_{L-1}}{z^{L-1}}$ is the filter's transfer function
- $U(z)$ is the *z*-transform of $u(n)$
- $Y(z)$ is the *z*-transform of $y(n)$

LMS must adjust the filter weights so that the error signal

$$e(n) = y_M(n) - y(n) = y_M(n) - \boldsymbol{w}(n)^T \boldsymbol{u}(n)$$

is minimized.

The criterion to minimize is

$$J(n) = e^2(n)$$

LMS updates the weight vector using the following law:

$$\boldsymbol{w}(n+1) = \boldsymbol{w}(n) + \frac{\mu}{2}\frac{\partial J(n)}{\partial \boldsymbol{w}(n)} = \boldsymbol{w}(n) - \mu \boldsymbol{u}(n) e(n)$$

where μ is the *convergence factor.*

- ✓ The gradient estimate is unbiased
- ✓ The expected value of the weight vector converges to $\boldsymbol{w^o}$ obtained with the minimization of the *Mean Square Error* criterion.

Grey-box methods
Model structure (1)

Grey-box model has structured parametrization derived from first principle approach:

- ✓ quadrotor is modeled as rigid body
- ✓ rotors aerodynamic terms from combined Momentum and Blade Element Theory

Pitch attitude dynamics on test-bed (all other DoF's constrained) is defined as

$$I_{yy}\dot{q}(t) = \frac{\partial M}{\partial q} q(t) + \frac{\partial M}{\partial u} u(t - \hat{\tau})$$
$$\dot{\theta}(t) = q(t)$$

where stability derivative of pitch moment M respect to angular rate q in hovering trim is

$$\frac{\partial M}{\partial q} = -2\rho A (\Omega R)^2 \frac{\partial C_T}{\partial q} d$$

Negative: aerodynamic damping

with $\frac{\partial C_T}{\partial q} = \frac{C_l/\alpha}{8} \frac{\sigma}{\Omega R}$

and control derivative of pitch moment (in hovering) is

$$\frac{\partial M}{\partial u} = \rho A_b (\Omega R)^2 \frac{\partial \, C_T/\sigma}{\partial \theta_R} d$$

Blade collective pitch

Adding a rotational mass-spring-damper (J,k,c) to modeling IMU vibration damping system (not negligible dynamics) through which the measuring device is connected to vehicle, equation become

$$
\begin{gathered}
I_{yy}\dot{q}(t) = \frac{\partial M}{\partial q} q(t) + \frac{\partial M}{\partial u} u(t-\hat{\tau}) + k(\theta_P(t) - \theta(t)) + c(q_P(t) - q(t)) \\
J\dot{q}_P(t) = -k\big(\theta_P(t) - \theta(t)\big) - c(q_P(t) - q(t)) \\
\dot{\theta}(t) = q(t) \\
\dot{\theta}_P(t) = q_P(t)
\end{gathered}
$$

where P subscript discern IMU from vehicle quantities.

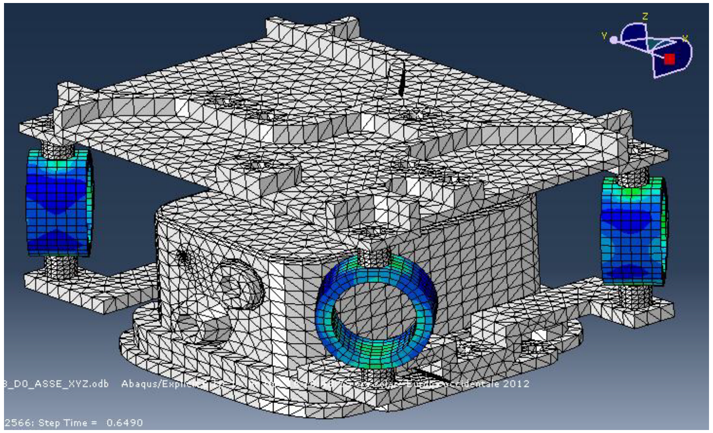

Rewriting the equations in state space form, continuous time LTI model is obtained

$$\dot{x}(t) = Ax(t) + Bu(t - \hat{\tau})$$
$$y(t) = Cx(t) + Du(t - \hat{\tau}) + v(t)$$

where the state vector is $x(t) = [q(t) \;\; q_P(t) \;\; \theta(t) \;\; \theta_P(t)]^T$ and matrices are

$$A = \begin{bmatrix} 1/I_{yy}\, \partial M/\partial q & -c/I_{yy} & -k/I_{yy} & k/I_{yy} \\ c/J & -c/J & k/J & -k/J \\ 1 & 0 & 0 & 0 \\ 0 & 1 & 0 & 0 \end{bmatrix} \qquad B = \begin{bmatrix} 1/I_{yy}\, \partial M/\partial u \\ 0 \\ 0 \\ 0 \end{bmatrix}$$

$$C = [0 \quad 1 \quad 0 \quad 0] \qquad D = [0]$$

The quadrotor moment of inertia I_{yy} was obtained from previously dedicated identification procedure, then the unknown parameters of structured model are

$$\Theta = \left(\frac{\partial M}{\partial q}, \frac{\partial M}{\partial u}, J, k, c \right)$$

Stability and control derivatives of pitch moment

IMU damping system model param.

Given sampled I/O dataset $\{u(t_i), y_M(t_i)\}$, $i \in [1, N]$
the ML estimate is equal to the value of Θ that maximizes the likelihood function, defined as the probability density function of y given Θ, *i.e.*

$$\mathbb{L}(y, \Theta) = P(y|\Theta)$$

$$\widehat{\Theta} = \arg\max_{\Theta} \mathbb{L}(y, \Theta)$$

In the case of a Gaussian $P(y)$, as the measurement noise $v(t)$, the ML estimator reduces to a least squares estimator, namely the cost function is

$$J(\Theta) = \frac{1}{N} \sum_{k=1}^{N} e(k, \Theta)^2$$

where $e(k, \Theta) = y_M(k) - y(k, \Theta)$.

The cost function minimum search is carried out through an iterative Newton-Raphson Method.

- SMI methods are more attractive than OE because of their non-iterative nature
- On SMI model is not possible to enforce a-priori knowledge of model structure, naturally allowed by grey-box approach

↓ bridge the gap between structured and unstructured model

Novel identification procedure proposed by *Bergamasco & Lovera 2013*

H_∞ model matching problem in frequency-domain, relating black-box unstructured model from SMI to structured one from first principle approach

Resulting non-convex, non-smooth optimization problem is solved exploiting computational tool developed by *Apkarian & Noll 2006*

(available in Matlab Robust Control Toolbox from R2012a → <hinfstruct>)

Attitude dynamics identification

Grey-box H_∞ approach

Unstructured LTI DT from SMI → convert to CT (zero order hold) →

$$\dot{x}(t) = A_{ns}x(t) + B_{ns}u(t)$$
$$y(t) = C_{ns}x(t) + D_{ns}u(t)$$

→ convert to tf in Laplace domain → $G_{ns}(s)$

Structured LTI CT from first principle

$$\dot{x}(t) = A_s(\Theta)x(t) + B_s(\Theta)u(t)$$
$$y(t) = C_s(\Theta)x(t) + D_s(\Theta)u(t)$$

→ $G_s(s,\Theta)$

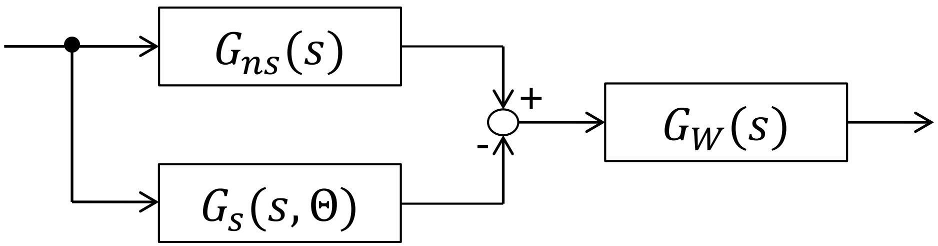

$$\hat{\Theta} = \arg\min_{\Theta} \| G_W(s)(G_{ns}(s) - G_s(s,\Theta)) \|_\infty$$

G_W is a suitable filter to focus the matching in the frequency range where $G_{ns}(s)$ well describes the real system, then in PRBS exitation spectrum

Since the time delay in system dynamics was removed before SMI, in structured model was set $\hat{\tau}$ = 0 for the model matching (and reintroduced later in validation)

Results introduction

- SMI algorithms parameter tuned to obtain higher VAF (Variance Accounted For) on cross-validation dataset
  - ✓ PI-MOESP: model order *n = 4 ;* Hankel I/O matrices rows n° *p = 40*
  - ✓ PBSID: model order *n = 5 ;* past / future window size *p / f = 11 / 7*

- OE ML approach does not offer specific parameters to be tuned

- H_∞ approach
  - ✓ filter G_W was tuned to reach best VAF performance on cross-validation dataset: adopted a 15th order low pass Butterworth, cut-off 7rad/s (complies with excitation spectrum peak)

Two different datasets were used for validation and performance comparison:

- Normal closed-loop operation of pitch attitude control system, representing typical flight condition
- Cross-validation: single PRBS excitation phase not employed in the identification process (dataset also used for algorithms parameters tuning)

Attitude dynamics identification
Results on closed-loop validation dataset

blue lines: measured pitch rate ; red dashed lines: models simulation

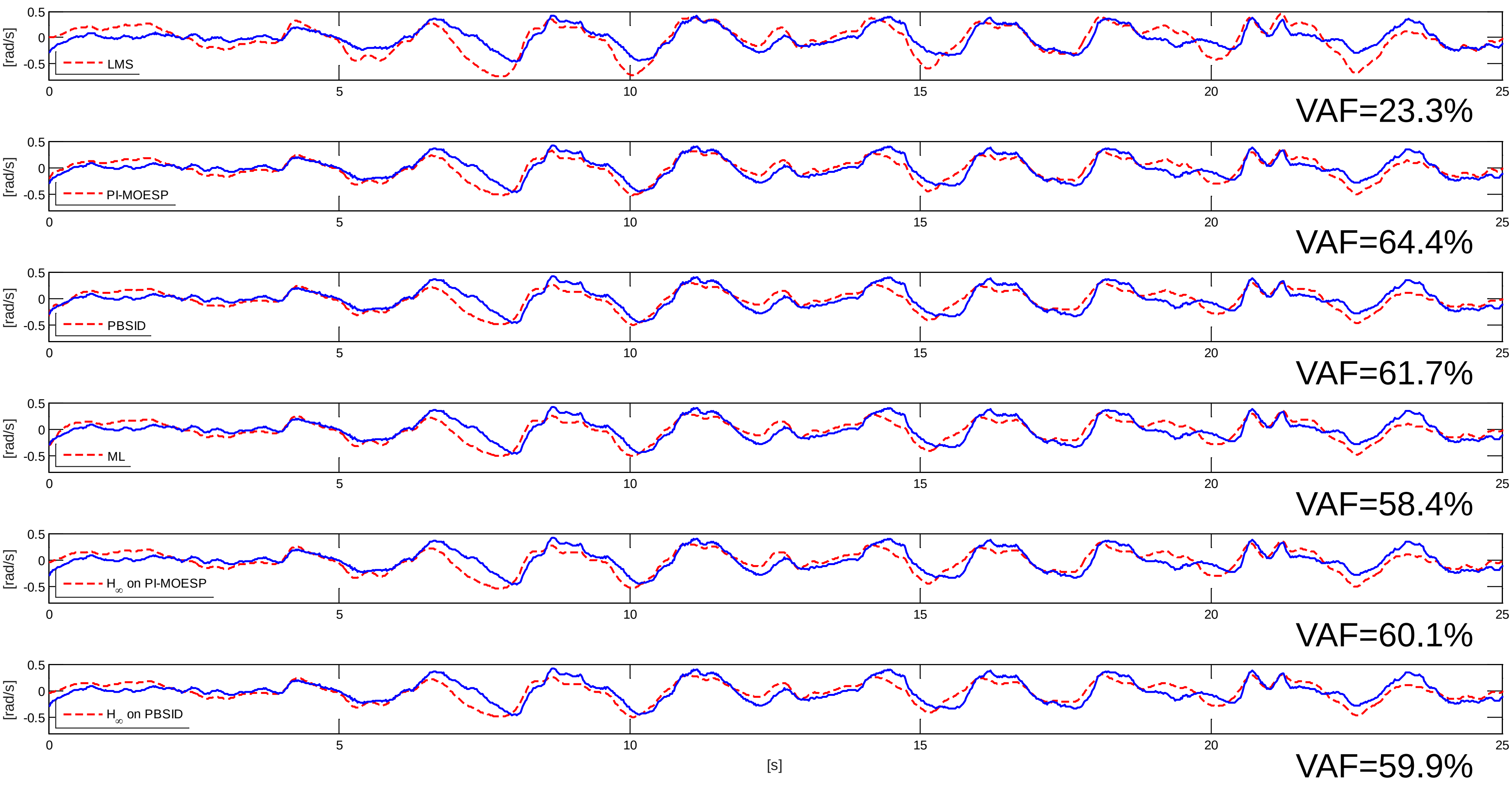

Attitude dynamics identification
Results on excitation cross-validation dataset

blue lines: measured pitch rate ; red dashed lines: models simulation

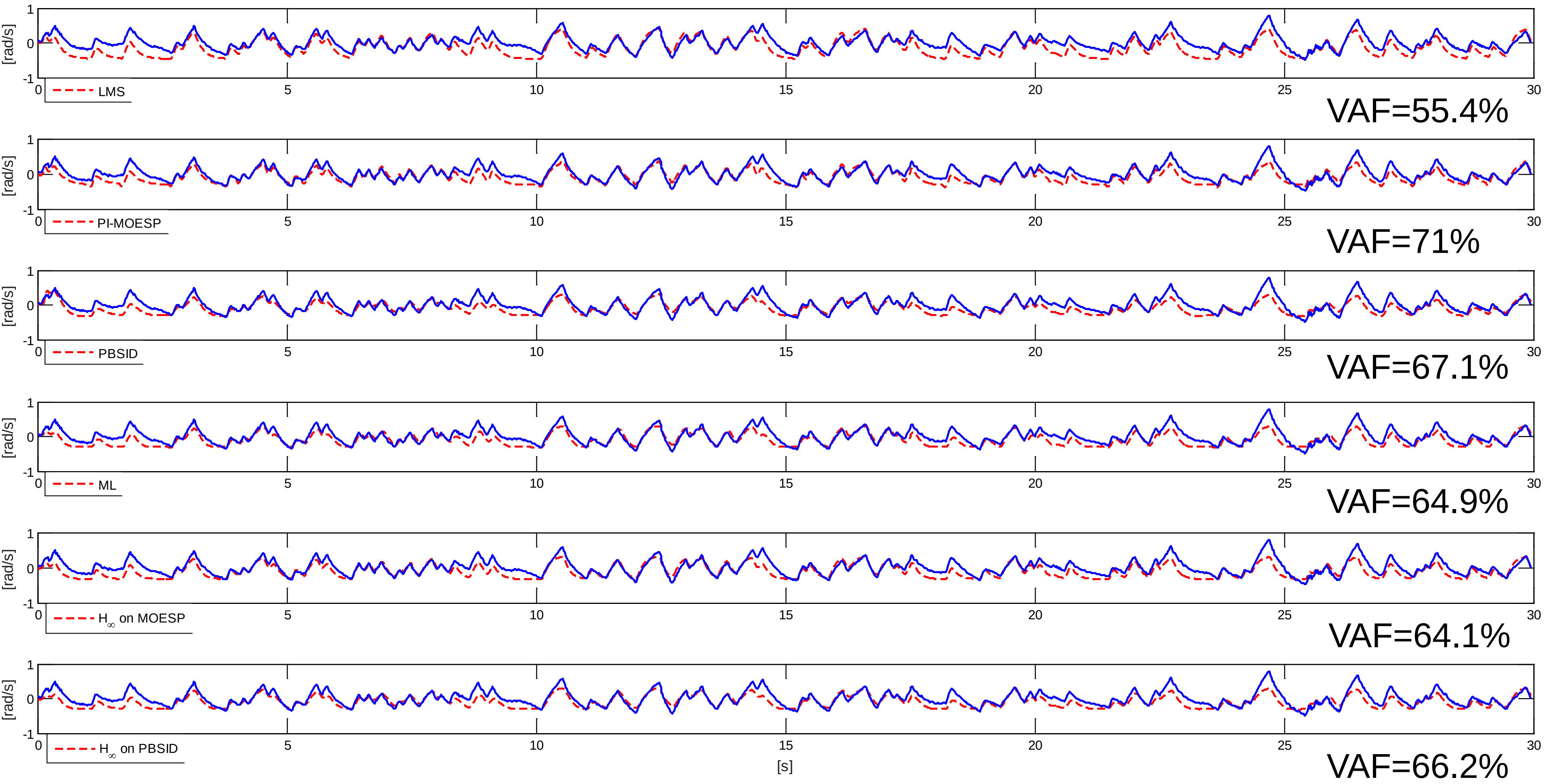

Attitude dynamics identification

Results: structured *vs.* unstructured models

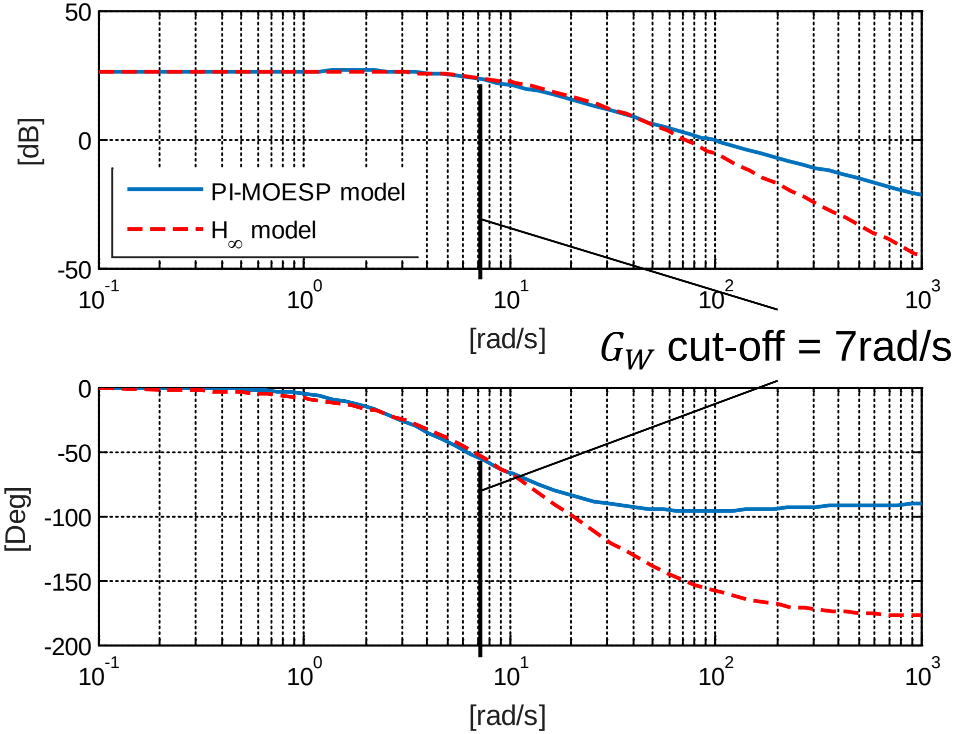

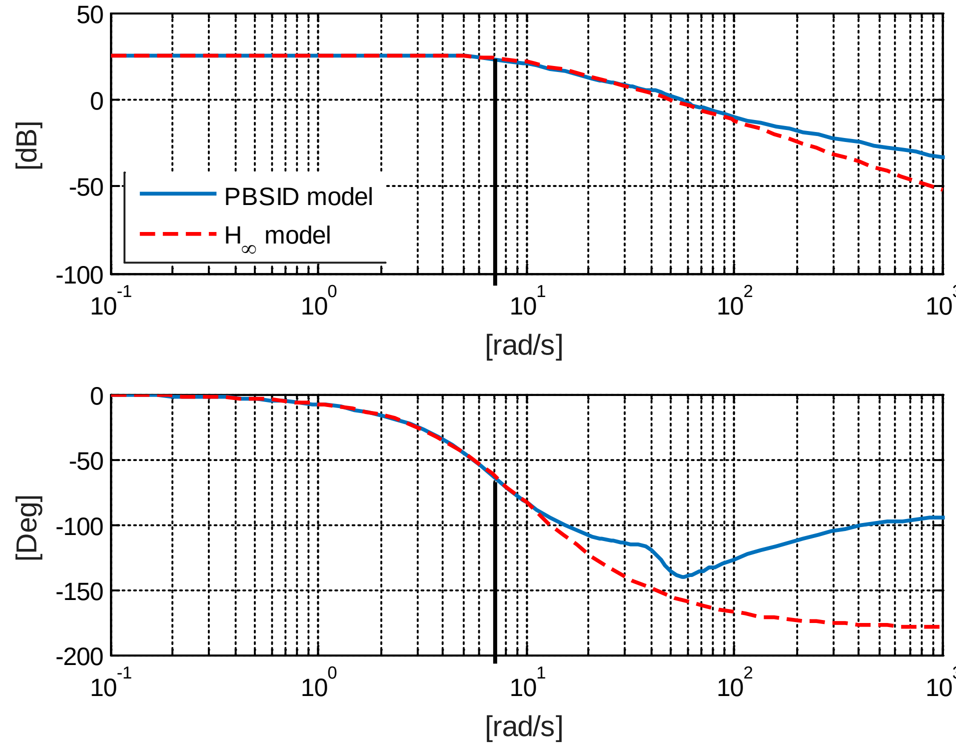

In time domain:

- H_∞ model *vs.* PI-MOESP, VAF = 96.9%
- H_∞ model *vs.* PBSID VAF = 99.6%

- Black-box models
  - LMS provides the worst result on both considered dataset: VAF on excitation cross-validation downgrades significantly on normal operation dataset (the model has poor generalization capability)
  - PI-MOESP guarantees the best VAF on both dataset : benchmark performance
  - PBSID is the second in rank but close to PI-MOESP

- Grey-box models
  - it is well known in the literature that leads to inferior performance respect to black-box (also for full-scale rotorcraft)
  - both OE ML and H_{∞} approach perform only slightly less satisfactorily than PBSID
  - H_{∞} approach model matches accurately the two SMI algorithms both in frequency and time domain

- Introduction and motivations
- Modelling and identification
- **Robust attitude control**
- Control design procedure test case
- Concluding remarks

Robust attitude control
Introduction

Quadrotor control synthesis has been studied extensively in the literature, adopting several approaches:

- ❑ PID architecture and LQ synthesis
- ❑ Robust control design
- ❑ Backstepping and Sliding mode
- ❑ Trajectory planning & tracking (e.g., adaptive control, dynamic inversion, flatness-based control, trajectory smoothing using motion primitives)

Concerning the control design part of the developed tool chain it was preferred to maintain the pre-existing on-board attitude controller scheme (cascade PID loops), in order to work in continuity and accelerating implementation process → structured H_∞ synthesis

The work focuses on near hovering condition:

- ✓ quadrotors mainly operate in this regime during typical missions
- ✓ in this operating mode the tighter handling qualities performance are required
- ✓ the attitude dynamics in hover can be replicated operating on a proper test-bed

Pitch angular velocity models comparison:
on test-bed *vs.* in flight (near hover), PI-MOESP *vs.* PBSID

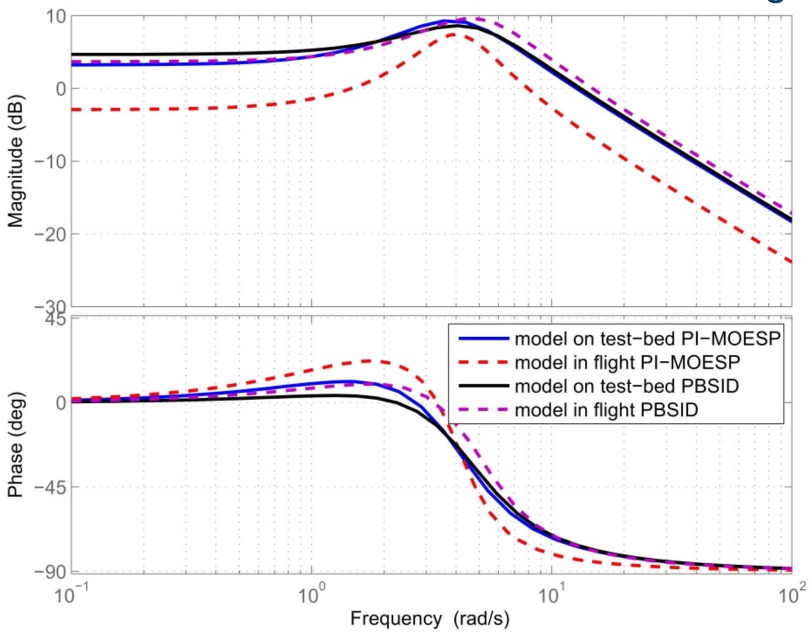

- ✓ PI-MOESP: poor agreement test-bed *vs.* flight
- ✓ Feedback action of supervision task added to PRBS is more invasive during in flight identification (quasi open-loop): avoid attitude angle limit overcoming in presence of wind disturbances
- ✓ PI-MOESP assumes feeding data gathered operating in open-loop

PBSID is able to deal with data generated in closed-loop

- ✓ PBSID: good agreement test-bed *vs.* flight
- ✓ PBSID close to PI-MOESP on test-bed data, when feedback action is less invasive (operations are nearest to be in open-loop)

PBSID on test-bed

$$\frac{q}{u} = \frac{12.517(s + 2.906)}{s^2 + 5.583s + 21.3}$$

n=2, p=35, f=6

PBSID in-flight

$$\frac{q}{u} = \frac{13.8194(s + 2.761)}{s^2 + 5.198s + 25.04}$$

n=2, p=f=5

Test-bed set-up is representative of the pitch attitude dynamics in hovering flight

Algorithm	ν-gap metric test-bed *vs.* flight	VAF test-bed	VAF flight
PI-MOESP	0.3405	65.8%	20.1%
PBSID	0.0741	65.1%	21.4%

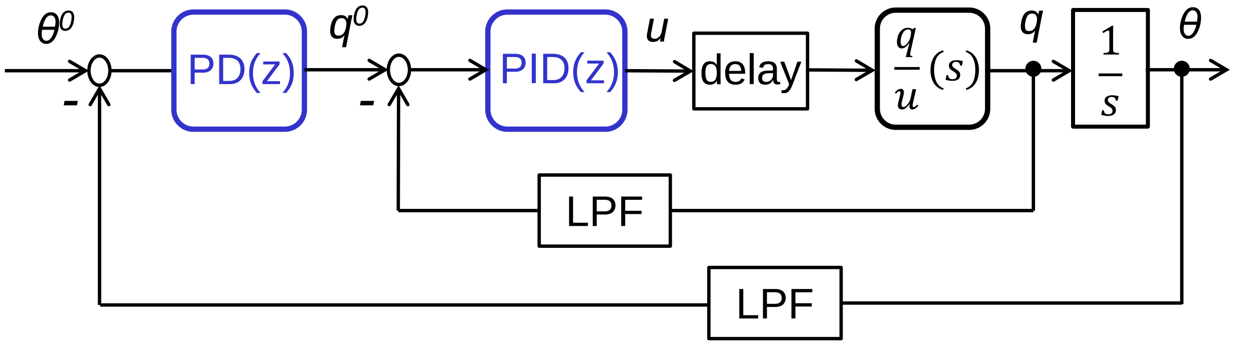

- Implemented accurate replica of pre-existing on-board controller in Simulink
- Cycle time 0.02 s

Pre-existing tuning from experimental trial & error manual process:

- ✓ guarantees adequate performance in terms of set-point tracking
- ✓ needs improvement in terms of wind gust rejection

Define proper requirements for H_∞ synthesis on fixed-structure controller

Performance channel

- Crossover frequency of each loop into specified bandwidth: 3.5→14 rad/s
- Set-point tracking target response time: 0.5 s
- Set-point tracking target maximum steady-state error: 0.001%

Robustness channel

- From process noise (wind gust) to control variable
- Disturbance rejection specified assigning maximum gain constraint function: high pass filter (gust is a low frequency noise), first order, gain 40 dB, cutting freq. 10 rad/s

Given

$P(s)$: real rational transfer matrix, PLANT

$K(\vartheta)$: STRUCTURED controller depending smoothly on a design parameter vector ϑ varying in space $\mathbb{R}^n$

Solve the optimization program

minimize $\|T_{w\to z}(P, K(\vartheta))\|_\infty$

subject to $\vartheta \in \mathbb{R}^n$: $K(\vartheta)$ stabilizes P internally

$T_{w\to z}(P, K(\vartheta))$: closed loop transfer function on considered I/O channel $w \to z$ on which requirements (performance and robustness) are defined

$P(s)$ regroups the process and the filter functions in loop shaping context

Resulting non-convex, non-smooth optimization problem is solved exploiting computational tool developed by *Apkarian & Noll, 2006*

Available in Matlab Robust Control Toolbox from R2012a → <looptune>

For the assigned controller structure, applied on identified models, the structured H_∞ algorithm finds the locally optimal parameters ϑ of the PIDs to satisfy desired requirements

	Controller parameter	Standard tuning	Optimal tuning: test-bed model	Optimal tuning: flight model
Outer loop on θ	K_p PD	9.26	5.4631	6.0491
	K_d PD	1.11	0.9376	1.0320
	T_f PD	0.03	0.0380	0.0377
Inner loop on q	K_p PID	0.257	0.3539	0.2986
	K_i PID	0.643	1.8562	1.6150
	K_d PID	0.0231	0.0084	0.0075
	T_f PID	0.0225	0.0430	0.0415

The standard tuning obtained through trial & error empirical procedure done manually was used as starting guess for the optimization procedure

Robust attitude control

Closed-loop functions

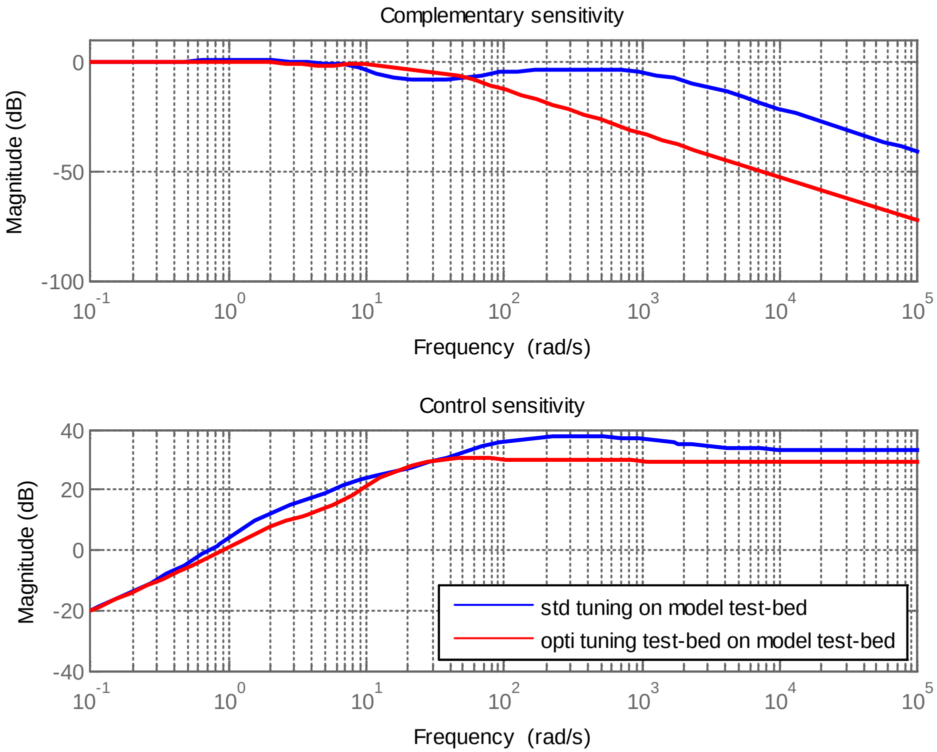

On test-bed model

In-flight model

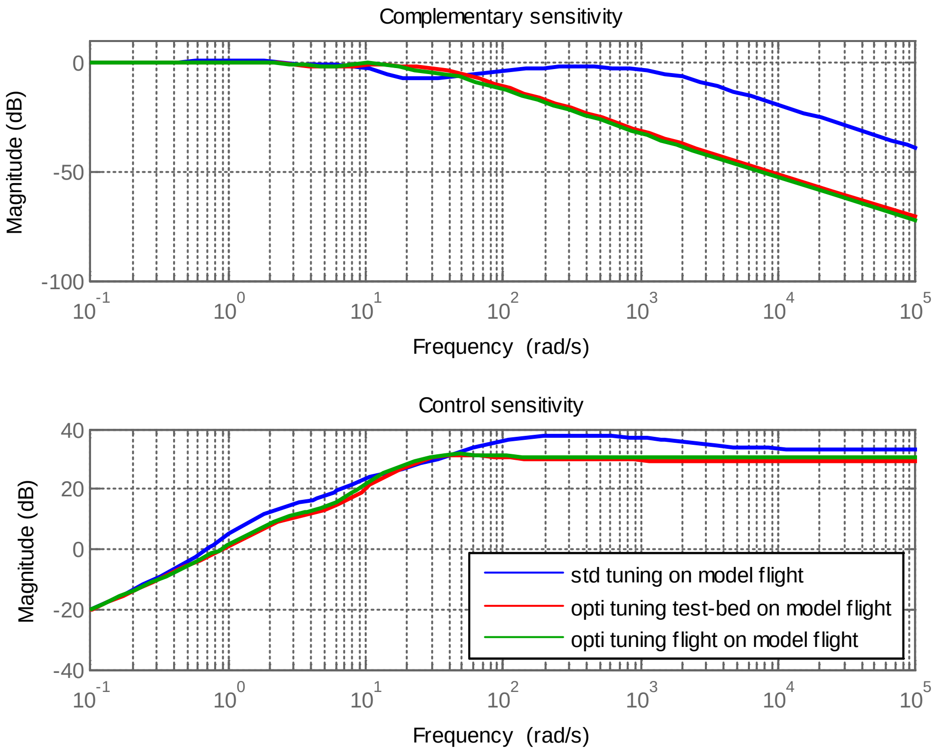

Robust attitude control
Simulation results: on test-bed model in the loop

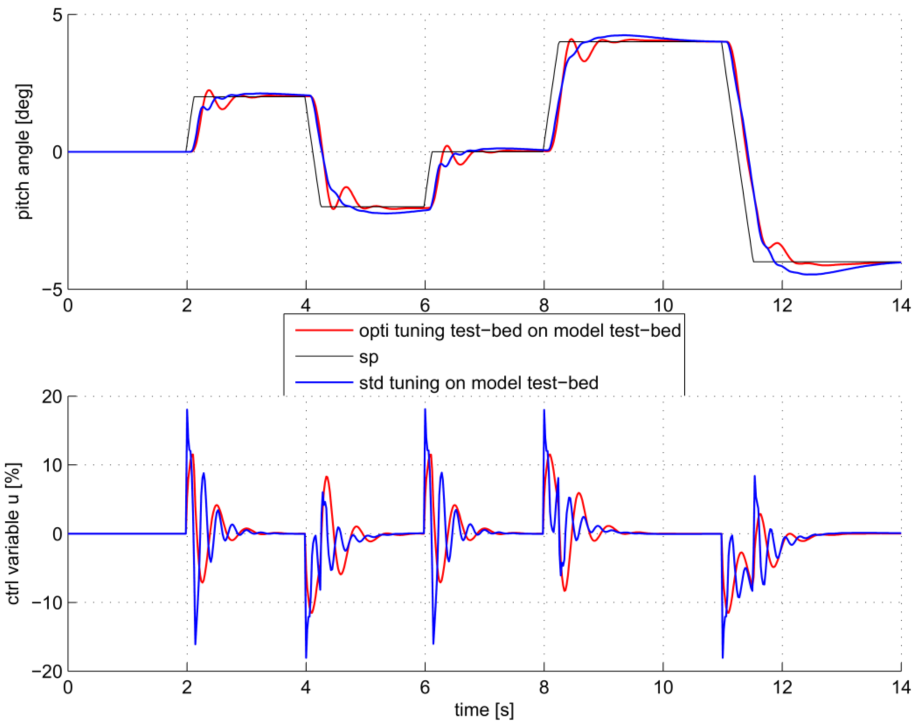

Pitch control variable saturation = ±30%

- ✓ Angular sp variation requested
- ✓ No process/measures noise
- ✓ Optimal tuning guarantees control effort reduction with similar/better tracking respect to standard

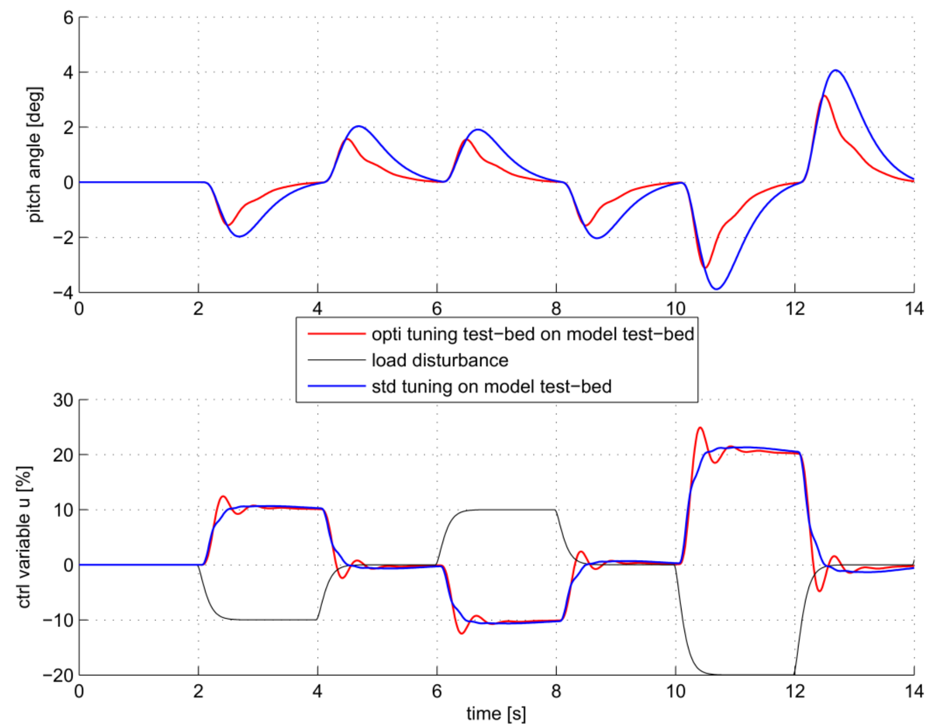

- ✓ Process disturbance, typical wind gust
- ✓ Angular sp null
- ✓ Optimal tuning guarantees angular drift reduction

Robust attitude control
Simulation results: in-flight model in the loop

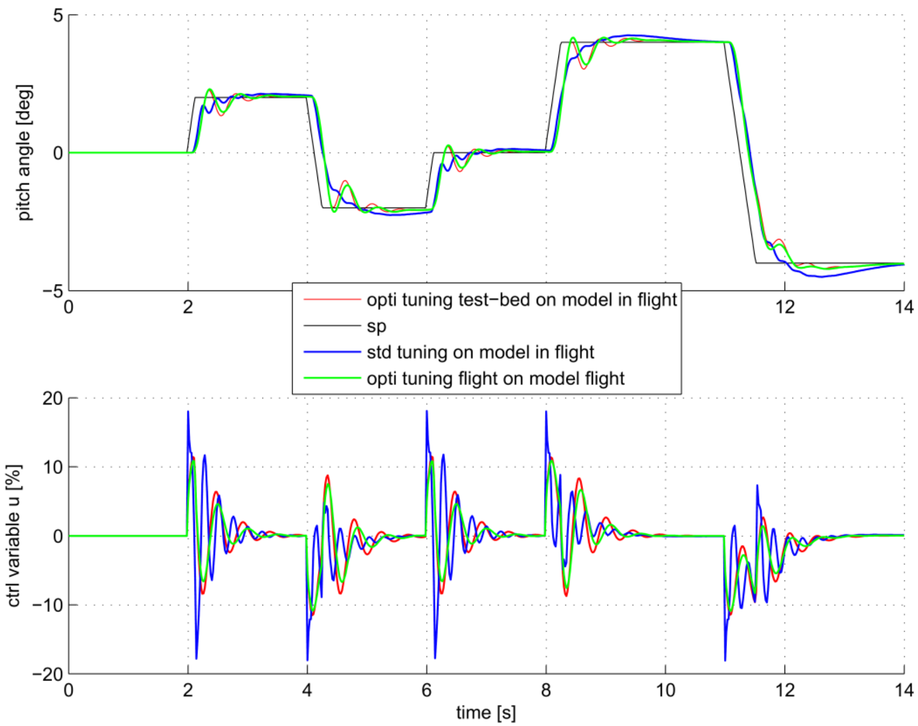

Pitch control variable saturation = ±30%

- ✓ Angular sp variation requested
- ✓ No process/measures noise
- ✓ Optimal tuning guarantees control effort reduction with similar/better tracking respect to standard
- ✓ Optimal tuning test-bed is close to flight one

- ✓ Process disturbance, typical wind gust
- ✓ Angular sp null
- ✓ Optimal tuning flight guarantees angular drift reduction
- ✓ Optimal tuning test-bed is close to flight one

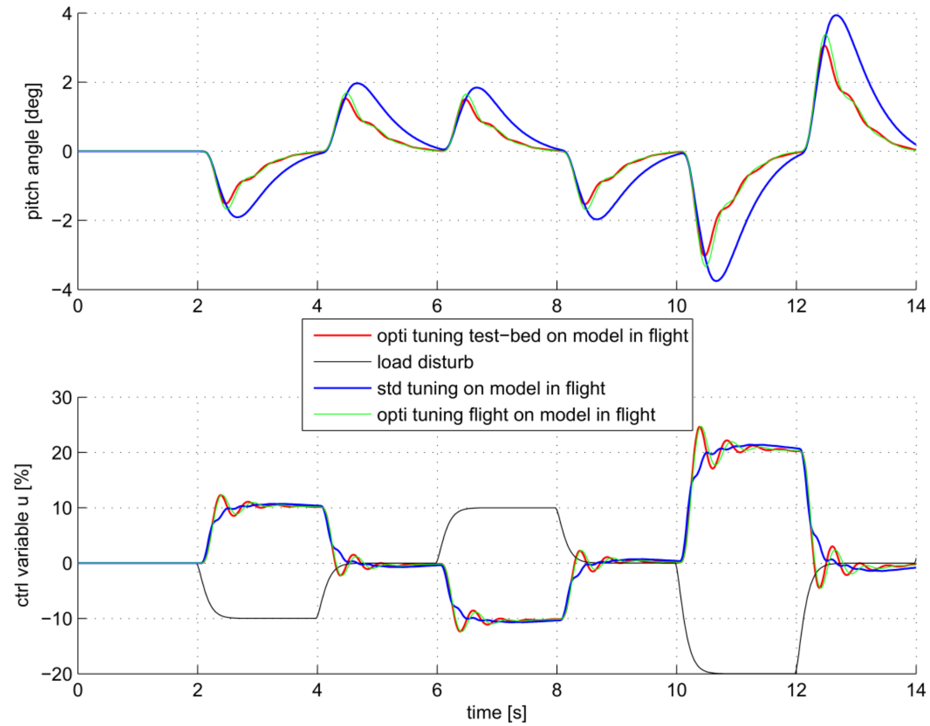

Robust attitude control
Experimental results on test-bed

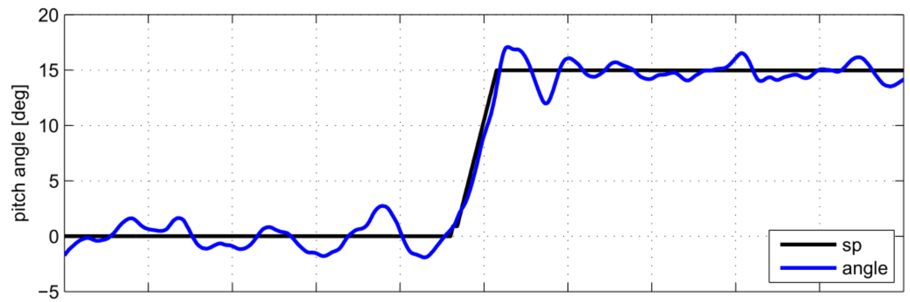

<u>Standard tuning</u>

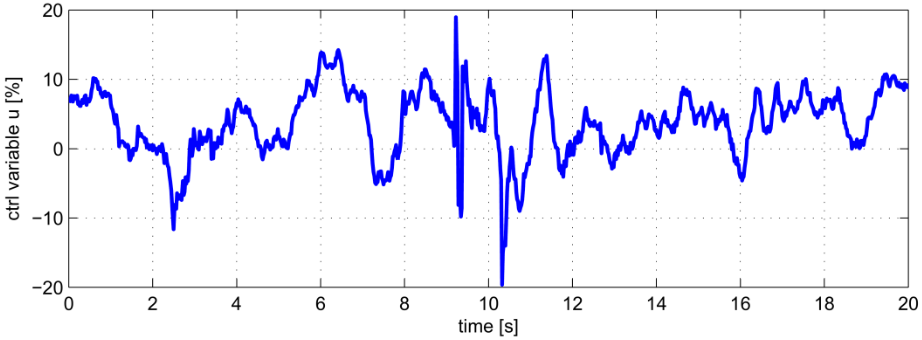

Pitch control variable saturation = ±30%

- ✓ Base throttle = 60% (hovering value)
- ✓ Angular sp variation requested
- ✓ Aerodynamic disturbances due to rotors wake recirculation in closed indoor test area

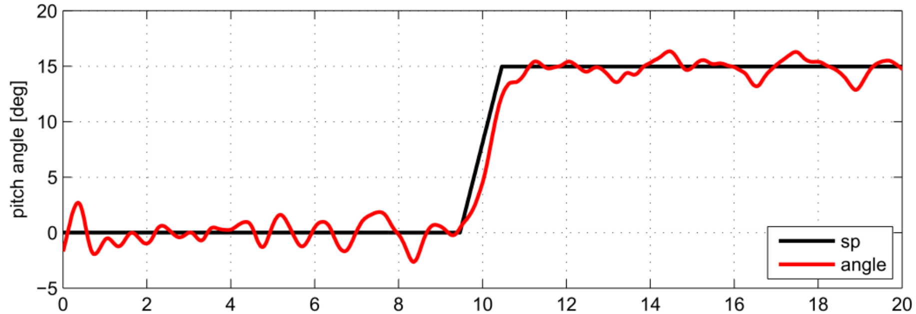

<u>Optimal tuning test-bed</u>

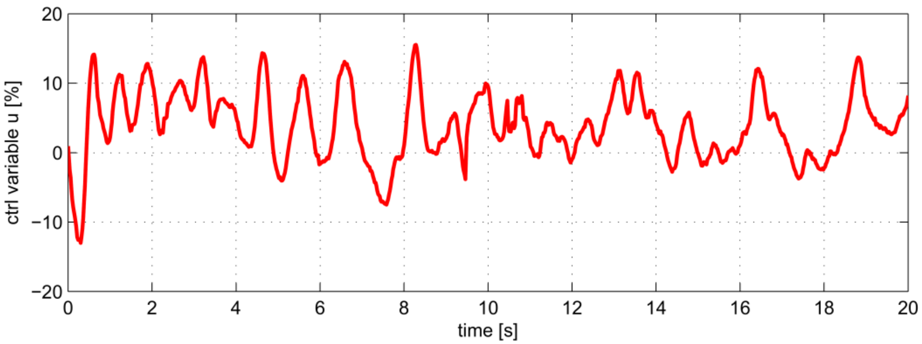

- ✓ Optimal tuning guarantees similar tracking performance with a reduction in control effort (confirming behavior from simulation)

Robust attitude control
PBSID models uncertainty (1)

Bootstrap based approach, 1000 replications

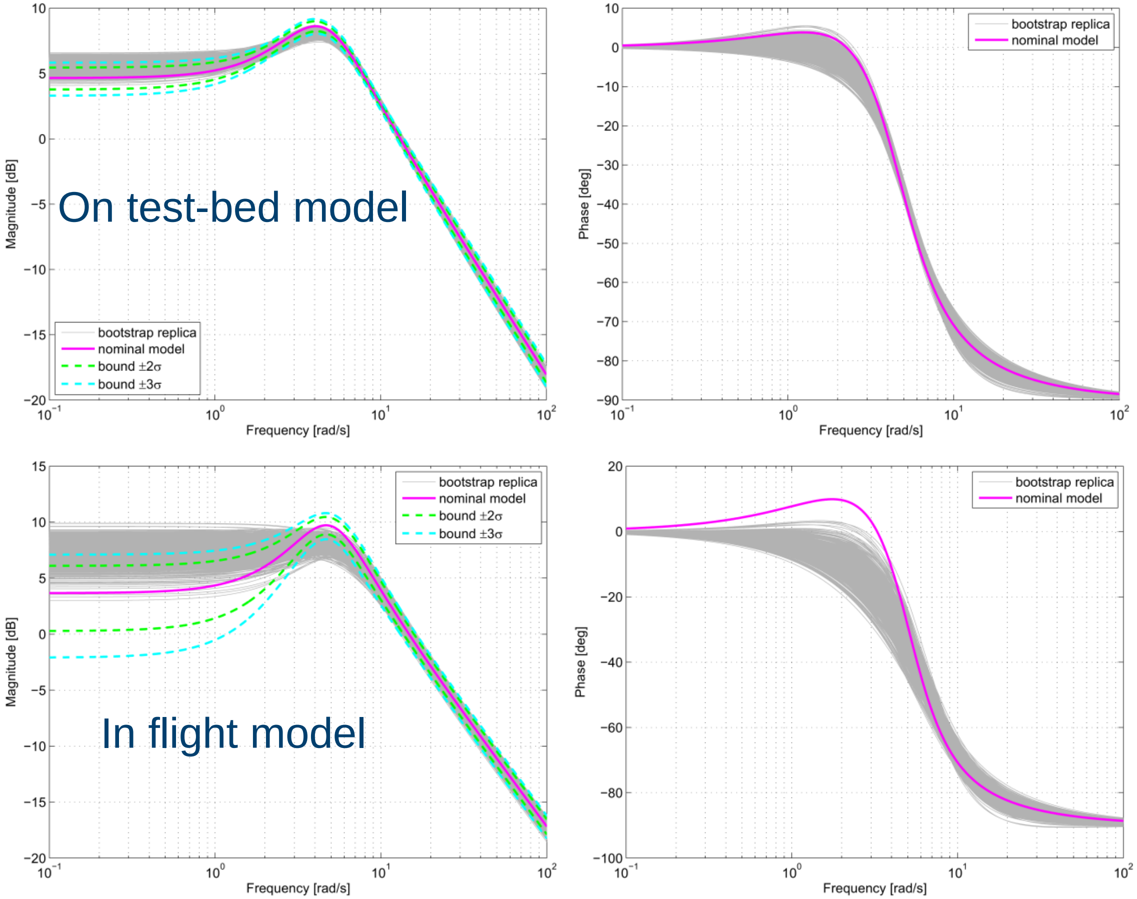

- ✓ On test-bed attitude pitch dynamics captured with very good accuracy
- ✓ Limited uncertainty band on all considered frequency range
- ✓ Especially narrow around PRBS excitation cut-off (7 rad/s)

- ✓ Identified model in flight presents a wider uncertainty band
- ✓ In design control bandwidth (3.5→14 rad/s) level of uncertainty can be considered acceptable

- ✓ The presence of wind gust implies a less repeatable test conditions w.r.t. identification in laboratory on test-bed
- ✓ In flight quadrotor attitude pitch dynamics is coupled with longitudinal one during the PRBS excitation, while on test-bed only the pitch rotation is allowed

Robust attitude control
PBSID models uncertainty (2)

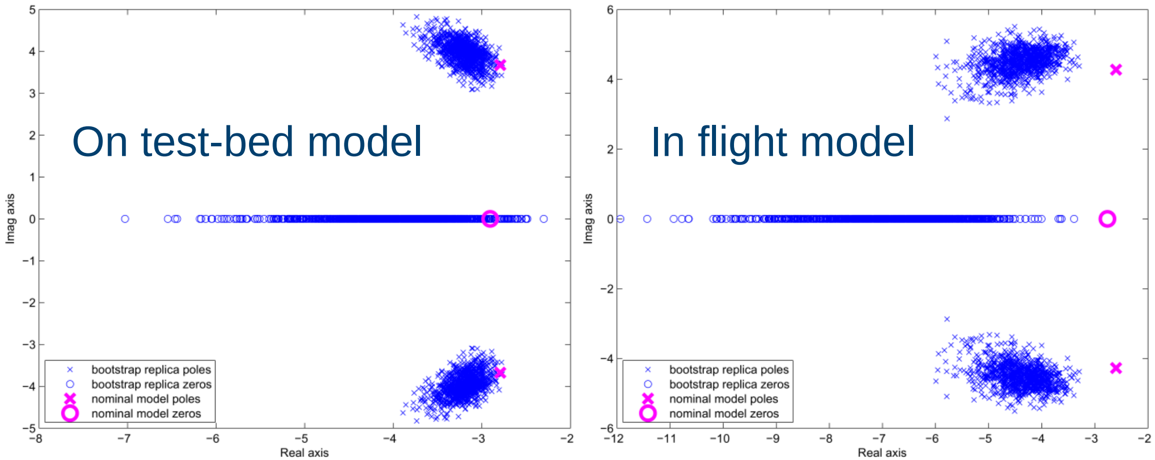

- ✓ Higher dispersion of real zero replicas w.r.t. to complex conjugate pole replications for both models
- ✓ Uncertainty of zero position is more significant because its nominal frequency is farther from excitation cut-off w.r.t. to nominal pole frequency

Bootstrap scheme for SMI (*Bittanti & Lovera, 2000*)

1. Estimate finite dimensional LTI nominal model (in innovation form) applying PBSID on original I/O dataset $(u(k), y(k))$
2. Calculate the model prediction error
3. Compute the covariance of prediction error and assume for it a Gaussian distribution
4. Generate *B* replications of original dataset, with $u^{*(i)}(k) = u(k)$ and $y^{*(i)}(k)$ obtained simulating the nominal model with input $u(k)$ and $e^{*(i)}(k)$, the latter generated re-sampling the Gaussian distribution of the residual
5. Estimate *B* replications of the nominal model applying PBSID to the *B* new dataset $(u^{*(i)}(k), y^{*(i)}(k))$

The number of replications required to obtain standard error convergence is usually very large, so the application of bootstrap is viable only for efficient identification algorithm

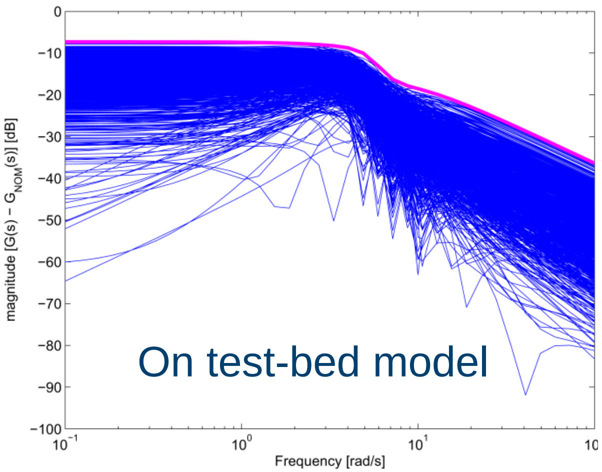

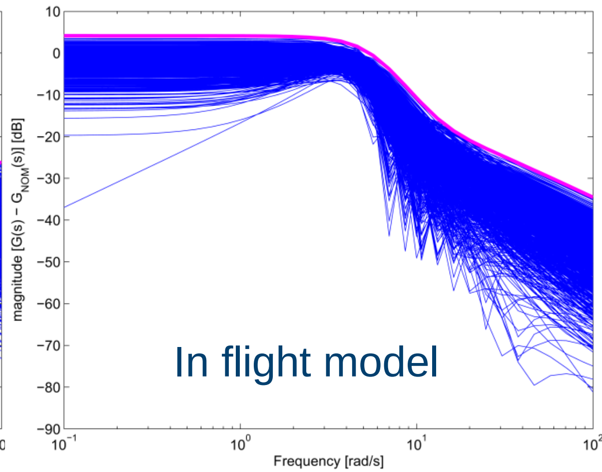

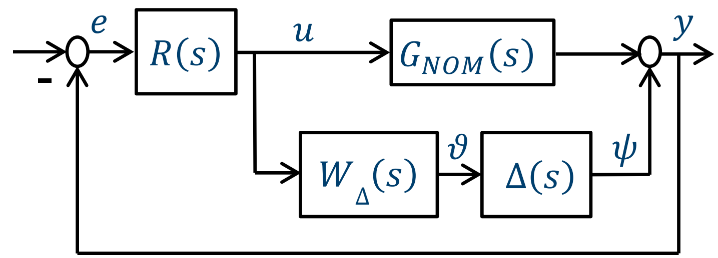

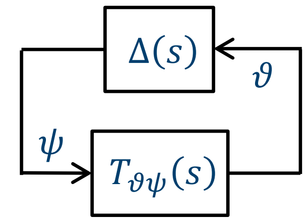

<u>Additive uncertainty</u>

$\mathcal{G} := \{G(s) = G_{NOM}(s) + W_{\Delta}(s)\Delta(s), \quad \|\Delta\|_{\infty} < h\}$

$\Delta(s)$: uncertainty LTI SISO random dynamics (with assigned peak gain)

$W_{\Delta}(s)$: stable, minimum phase, shaping filter, order 3

$if\ \|\Delta\|_{\infty} < 1, \qquad |G(j\omega) - G_{NOM}(j\omega)| = |\Delta(j\omega)W_{\Delta}(j\omega)| < |W_{\Delta}(j\omega)|, \forall\omega$

Tuning	Process	h_{lim}
Standard	test-bed	0.370
	flight	0.114
Optimal on test-bed	test-bed	0.600
	flight	0.189
Optimal in flight	flight	0.173

The control system can be represented by the *two level scheme*

$$T_{\vartheta\psi}(s) = \frac{W_{\Delta}(s)R(s)}{1 + R(s)G_{NOM}(s)} = W_{\Delta}(s)V_{NOM}(s)$$

From *small gain theorem* the <u>c.l.s. is stable</u> $\forall\ \Delta(s) \in \mathcal{H}_{\infty}$ (*i.e.* a stable t.f) with $\|\Delta\|_{\infty} < \left(\|T_{\vartheta\psi}\|_{\infty}\right)^{-1}$, hence

$h_{lim} = (\|W_{\Delta}(s)V_{NOM}(s)\|_{\infty})^{-1}$ where $V_{NOM}(s)$ is the nominal control sensitivity

Robust attitude control

Monte Carlo simulation results – on test-bed model

Uncertainty block with imposed peak gain equal to robust stability limit h_{lim}, randomly sampled to generate 1000 Monte Carlo simulations

Set-point change

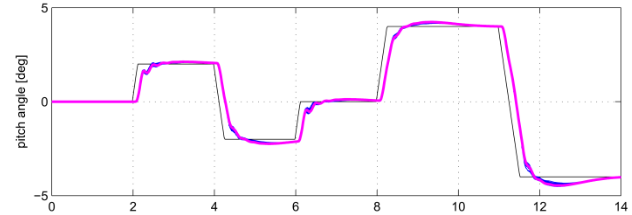

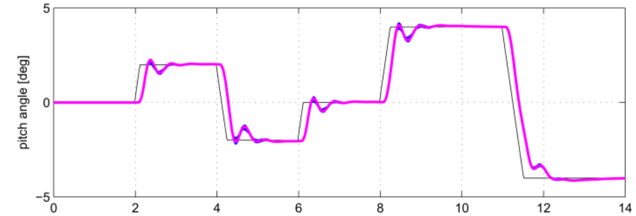

Standard tuning

Optimal tuning test-bed

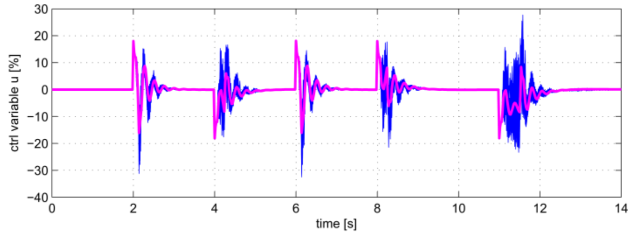

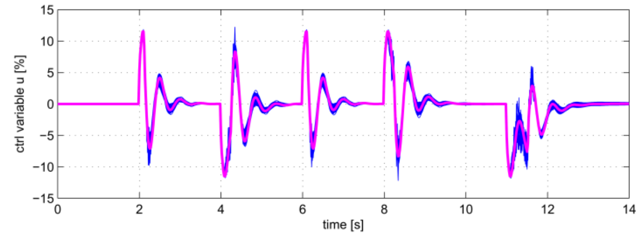

Load change

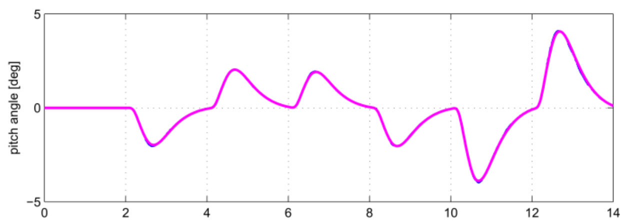

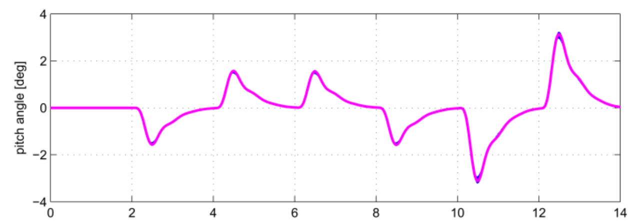

Standard tuning

Optimal tuning test-bed

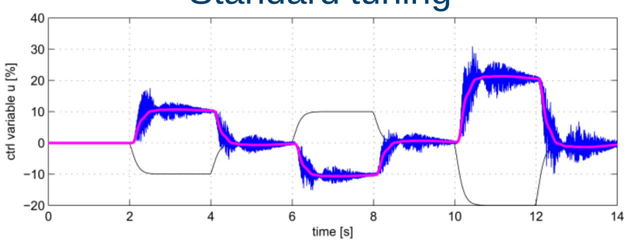

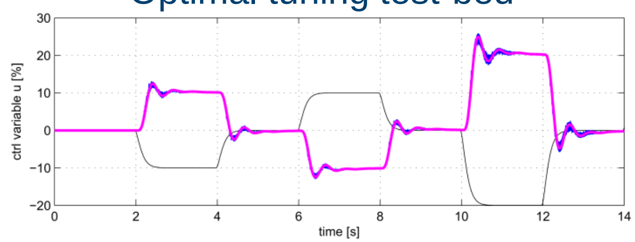

Magenta line: nominal model

Blue lines: uncertain models

Robust attitude control
Monte Carlo simulation results – in flight model

Set-point change

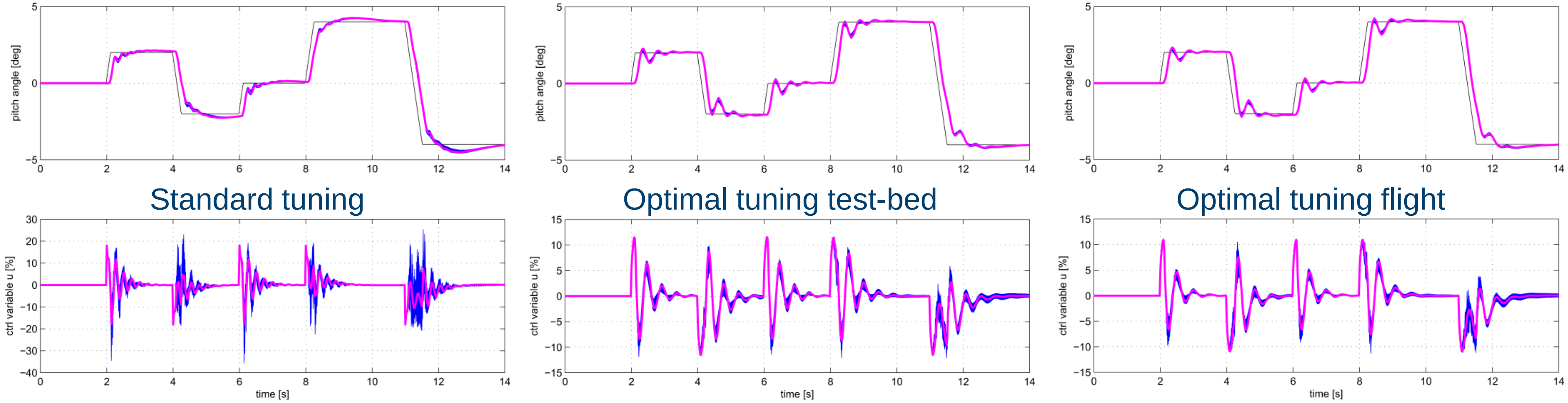

Load change

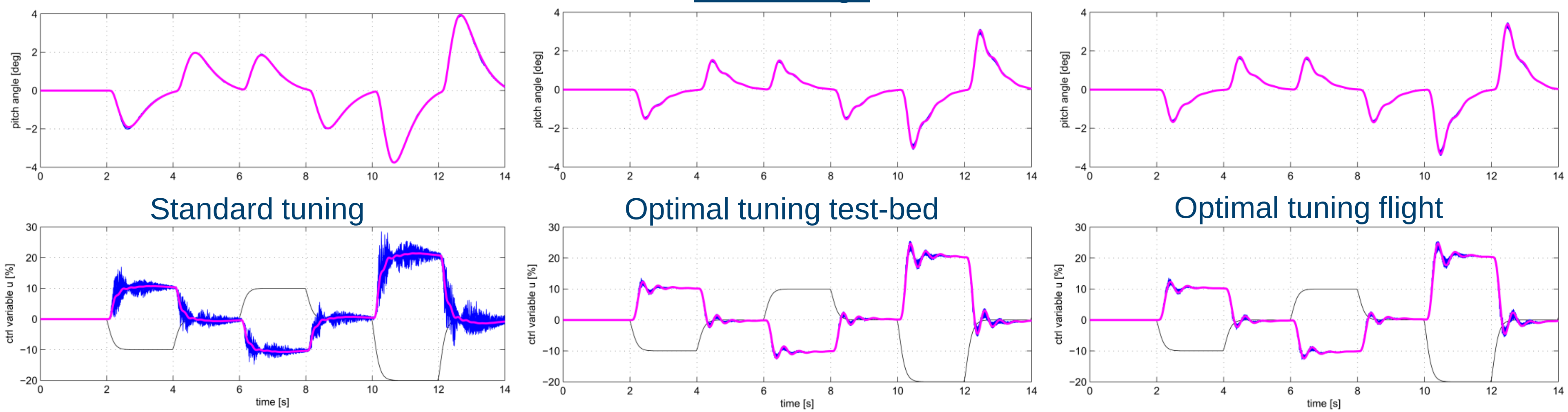

- Introduction and motivations
- Modelling and identification
- Robust attitude control
- **Control design procedure test case**
- Concluding remarks

Control design procedure test case
Introduction

- The proposed attitude control design procedure (and the relative tool-chain), from identification conducted indoor on single DoF test-bed, to the structured H_∞ synthesis, was applied to the production Aermatica quadrotor

- It is a tight test case, aimed to strengthen procedure validity, considering the <u>significant increment in quadrotor size/weight</u> w.r.t. adopted prototype for the development

ANTEOS A2-MINI/B

- ✓ Variable collective pitch
- ✓ MTOW = 9 kg (+80%)
- ✓ Rotors radius = 0.375 m (+39%)
- ✓ Arms length = 0.629 m (+51%)

Control design procedure test case
Identification experiments (1)

- ✓ Single DoF (pitch) test-bed (rotors in OGE)
- ✓ PRBS excitation signal
- ✓ Experiments carried out in quasi open-loop conditions
- ✓ <u>None in flight identification campaign was conducted</u>

PRBS parameters tuning:

- ✓ expected dominant attitude dynamics range: 3 to 7 rad/s (lower w.r.t. to P2-A2 prototype)
- ✓ necessary greater pitch control command % w.r.t. to P2-A2

Identification campaign	PRBS switching time range [s]
1	0.05 – 0.1
2	0.1 – 0.2
3	0.2 – 0.4
4	0.4 – 0.8

PRBS amplitude	Blade pitch command difference between opposite rotor [%]
1	± 11
2	± 13
3	± 15

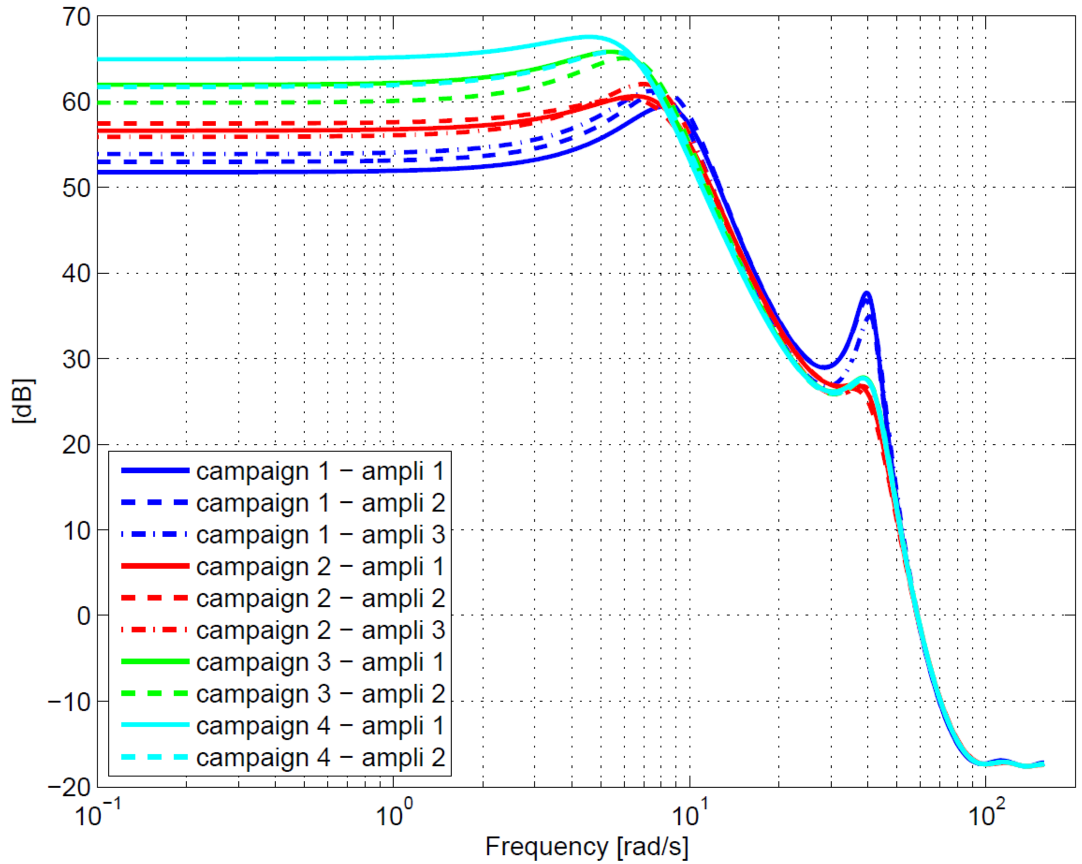

Control design procedure test case
Identification experiments (3)

Identification input signal obtained concatenating 2 excitation segments from different test in order to average out mild non-linearities

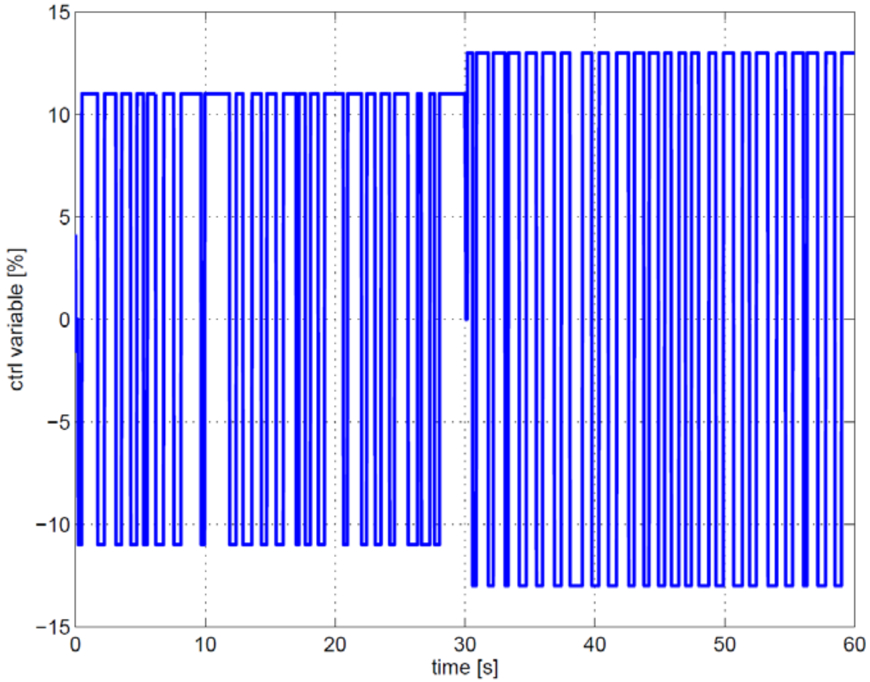

Data logged during test @ 50Hz

Input: pitch attitude control variable

Output: $\theta, q, \dot{q}$ from on-board IMU

Excitation spectrum

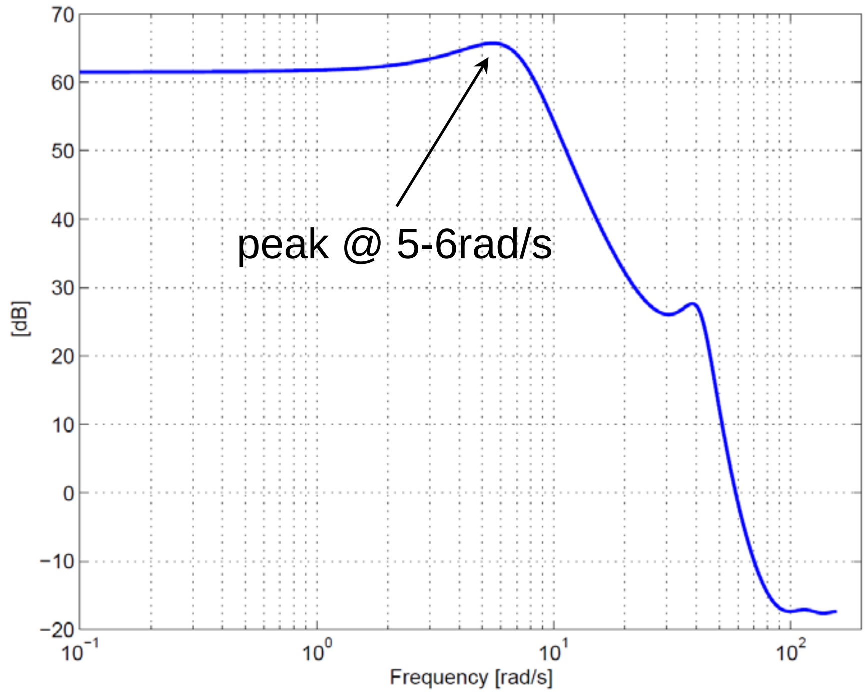

Control design procedure test case
Identification results (1)

Adopted the black-box approach → subspace method → PI-MOESP algorithm

SISO model from ctrl input u to pitch angular rate $q \rightarrow \frac{q}{u} = \frac{10.29s+33.68}{s^2+5.112s+14.72}$ $(n = 2, p = 39)$

Model order fixed, block-size p of Hankel data matrices tuned to obtain higher VAF on cross-validation dataset

System dynamics time delay ($\hat{\tau}$ = 0.06s) in SMI properly considered

As expected dominant dynamics become slower increasing the vehicle dimensions:

- ✓ complex conjugate poles frequency decreases from 4.09 to 3.67 rad/s
- ✓ poles damping factor increases from 0.567 to 0.697
- ✓ real zero frequency moves from 2 to 2.4 rad/s

passing from P2-A2 to A2-MINI/B

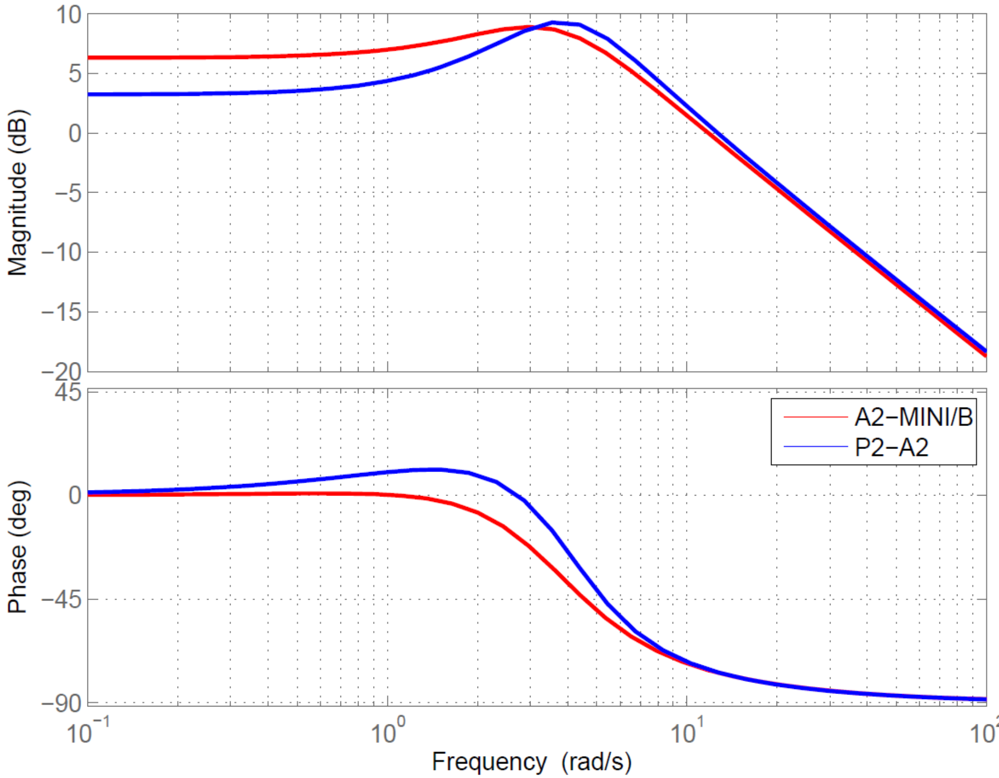

Control design procedure test case
Identification results (2)

A2-MINI/B identified pitch model performance:

- ✓ Cross-validation dataset (PRBS not used for identification) → VAF = 83.13%
- ✓ Validation dataset (normal control, pitch angle sp variation) → VAF = 61.22%

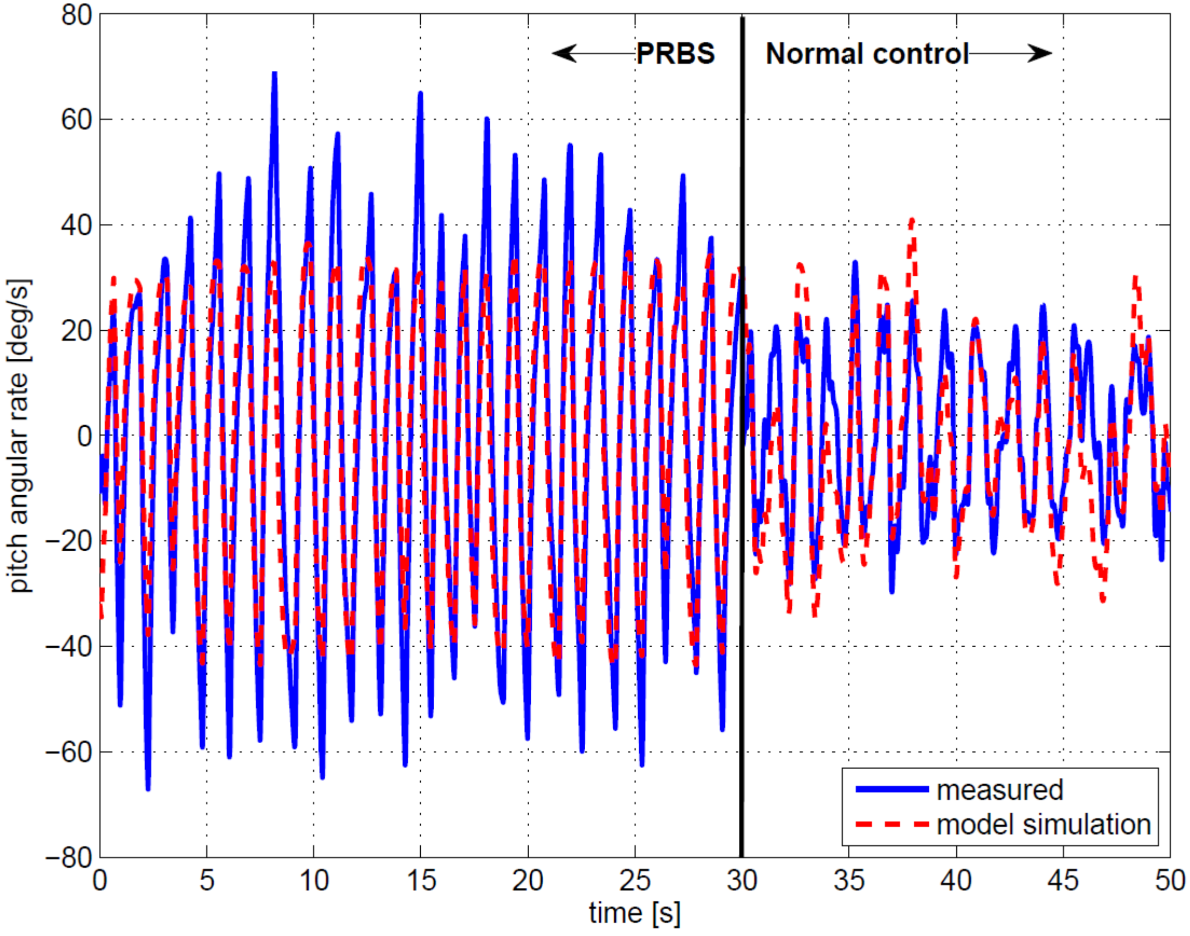

Control design procedure test case
H_∞ synthesis requirements for pitch attitude ctrl (1)

The A2-MINI/B has the same attitude ctrl architecture of the P2-A2, based on decoupled cascaded PID loops for the pitch, roll and yaw axes (cycle time 0.02 s)

Instead of standard PIDs, A2-MINI/B adopts PIDs 2 dof, with the additional parameters:
- ✓ proportional set-point weight b : varying from 0 to 1 (std PID b=1)
- ✓ derivative set-point weight c : flag equal to 0 or 1 (std PID c=1)

The pre-existing attitude tuning (from experimental trial & error manual process) was extensively tested in flight hence the desired qualitative performance improvements are:

- ✓ better set-point tracking: response time is almost adequate while a reduction of settling time and oscillation amplitude around the angular sp is needed
- ✓ better wind gust rejection capability in terms of maximum angular drift and reduction of oscillation in recovery the desired angular sp

H_∞ synthesis requirements for pitch attitude ctrl (2)

From qualitative to quantitative requirements for H_∞ synthesis on assigned fixed-structure controller

Performance channel

- Crossover frequency of each loop into specified bandwidth: 4→16 rad/s
- Set-point tracking target response time: 0.3 s
- Set-point tracking target maximum steady-state error: 0.001%

Robustness channel

Disturbance rejection specified assigning a gain constraints as function of frequency → high pass filter

- maximum gain of -3 dB above the cutting frequency (at 0.5 rad/s)
- 60 dB/decade roll-off below 0.5 rad/s

Control design procedure test case

Optimal tuning parameters (pitch attitude controller)

Outer loop on θ

Inner loop on q

Controller parameter	Standard tuning	Optimal tuning
K_p PD	15.1515	19.8566
K_d PD	1.9697	1.5331
T_f PD	0.0325	0.0723
b PD	1	0.9986
c PD	0	0
K_p PID	0.3691	0.5253
K_i PID	2.0504	1.7525
K_d PID	0.0183	0.0144
T_f PID	0.0124	0.0206
b PID	0.46	0.5787
c PID	1	1

c flag NOT optimized, set equal to standard tuning

The standard tuning was used as starting guess for the optimization procedure

Control design procedure test case
Closed-loop functions

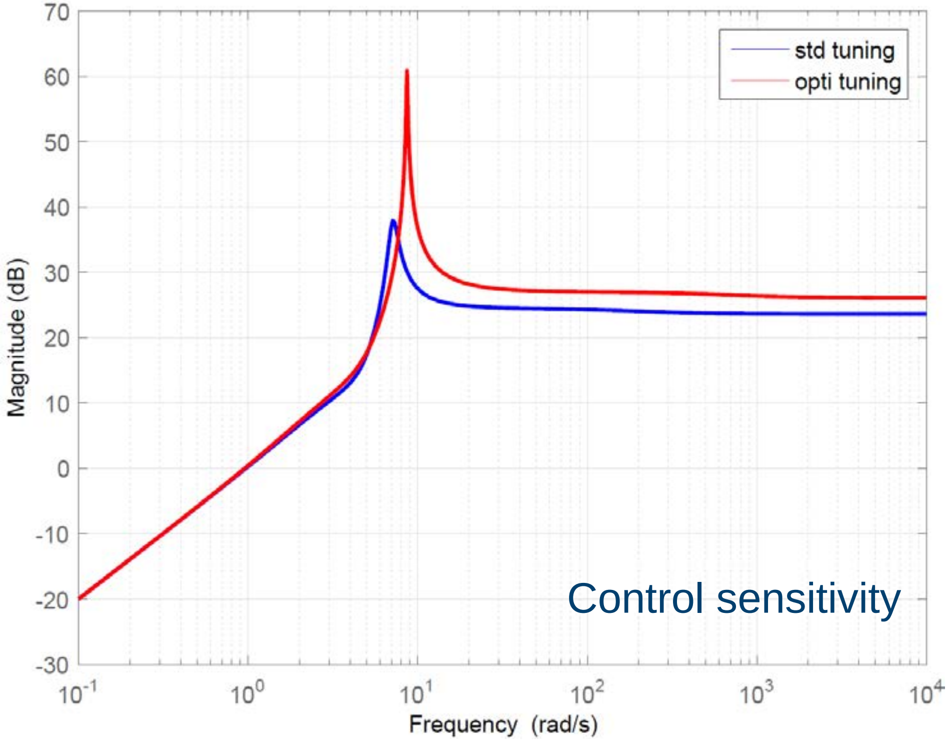

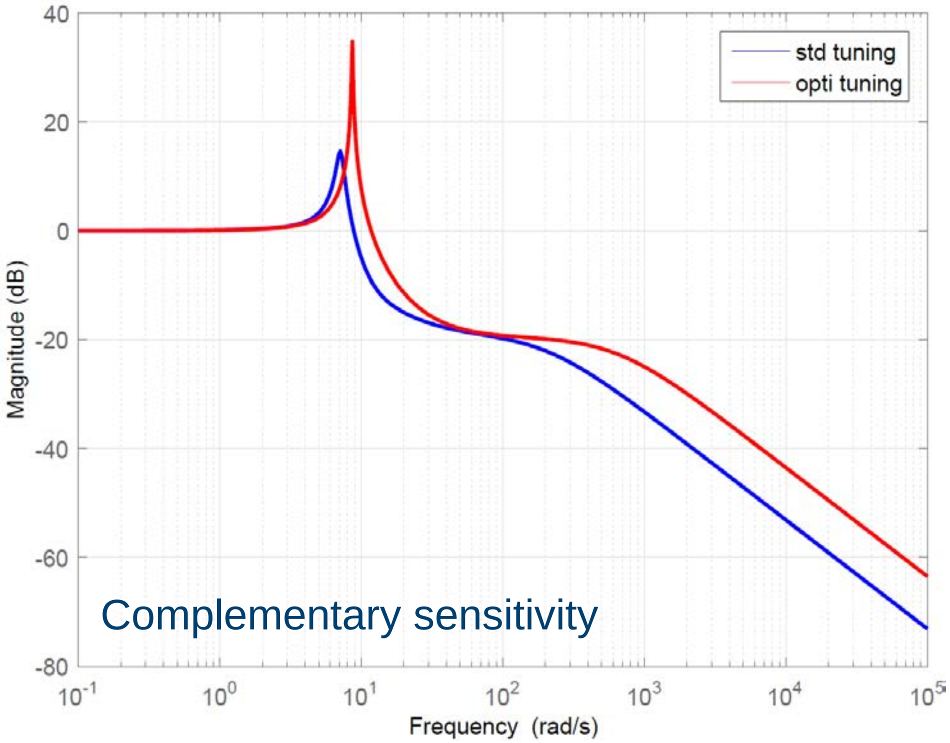

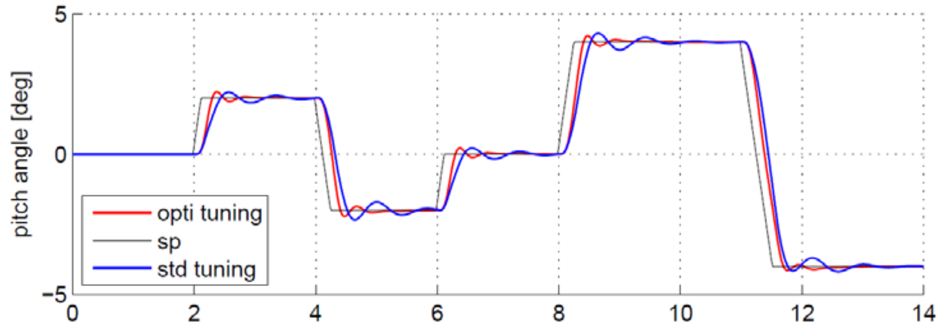

- Angular sp variation requested
- No process/measures noise
- Pitch control variable saturation = ±30%

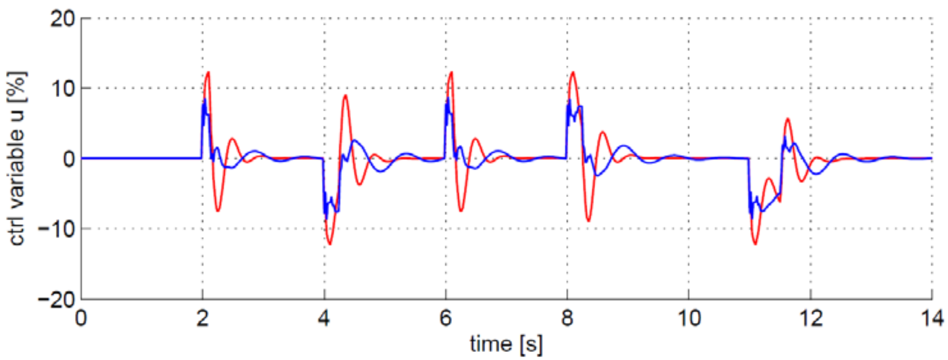

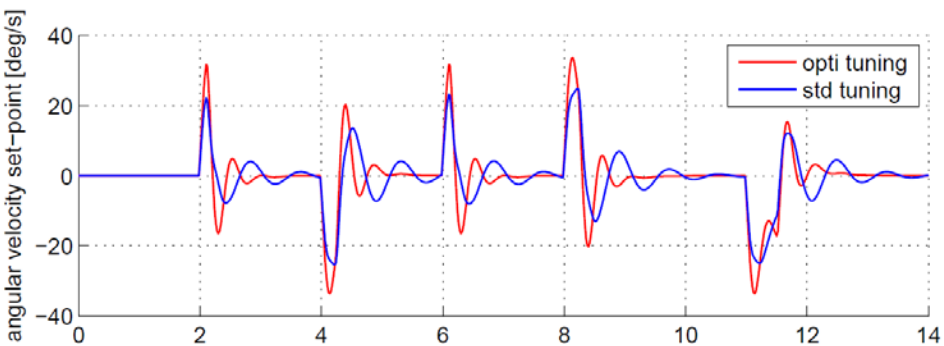

Opti tuning shows w.r.t. std one:

- ✓ reduced settling time (less oscillation on sp)
- ✓ response time slightly lower with non significant overshoot increment
- ✓ control effort increase (of an acceptable amount)

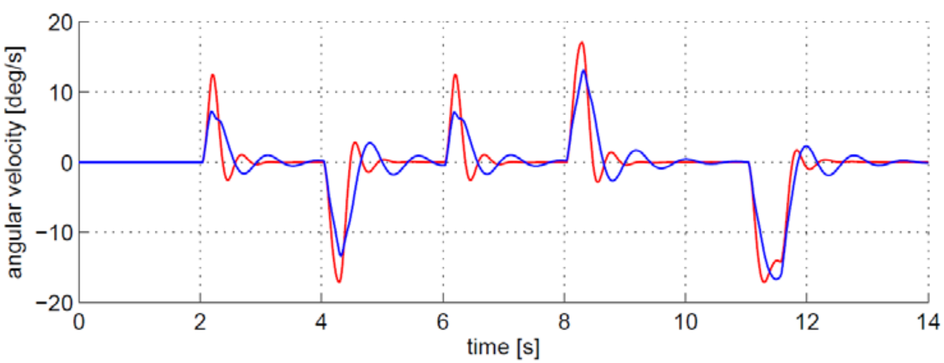

Control design procedure test case

Simulation results (load disturbance)

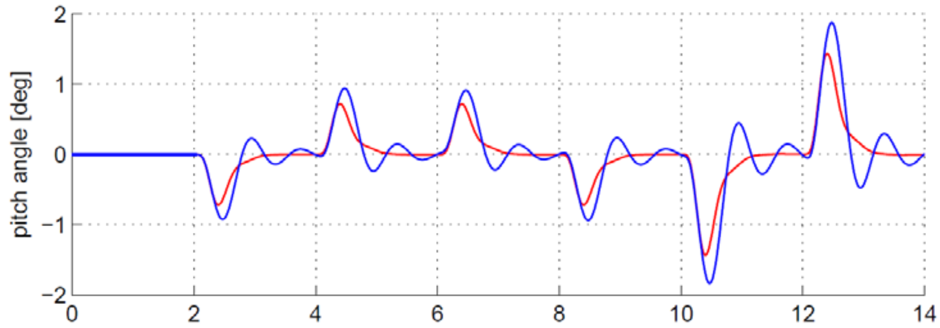

- Process disturbance, typical wind gust
- No measures noise
- Angular sp null
- Pitch control variable saturation = ±30%

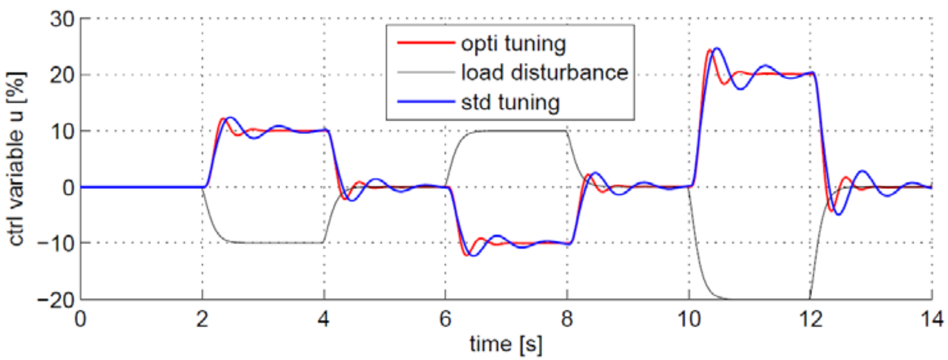

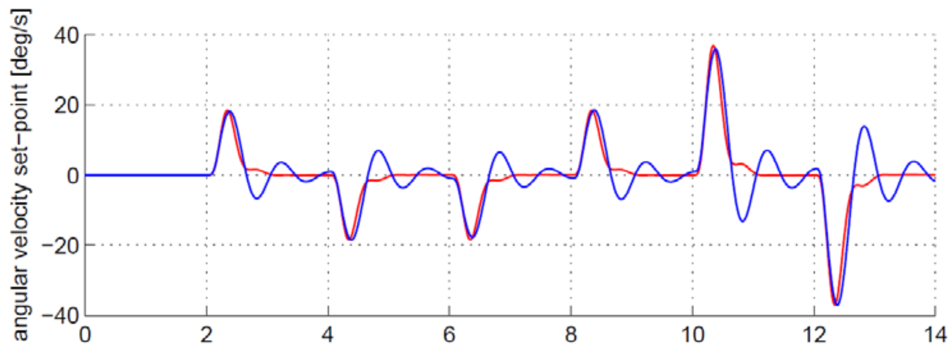

Opti tuning shows w.r.t. std one:

- ✓ reduced drift from null angular sp due to gust
- ✓ pitch angle oscillations in sp recovery eliminated

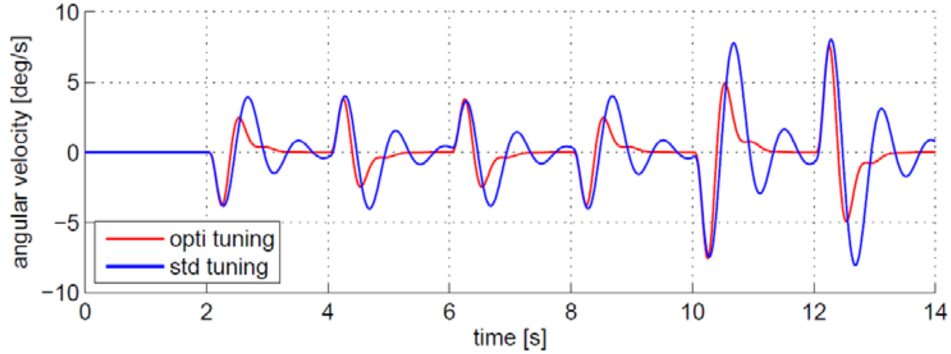

Control design procedure test case
Model uncertainty analysis

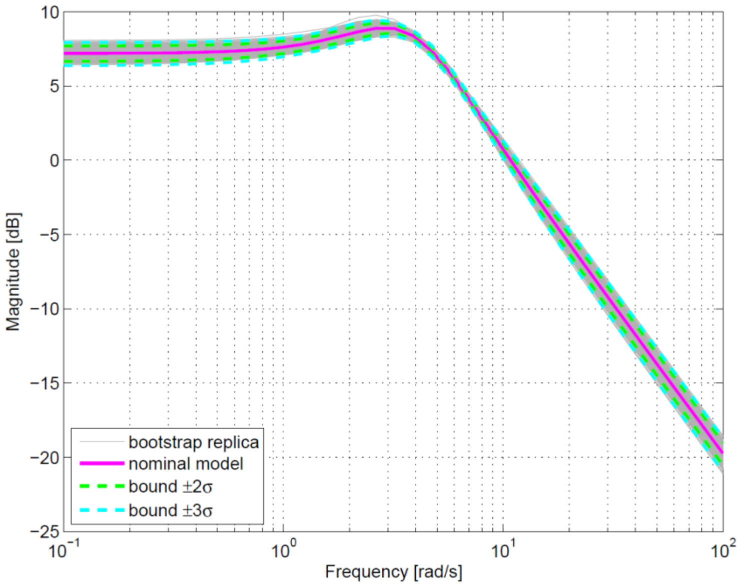

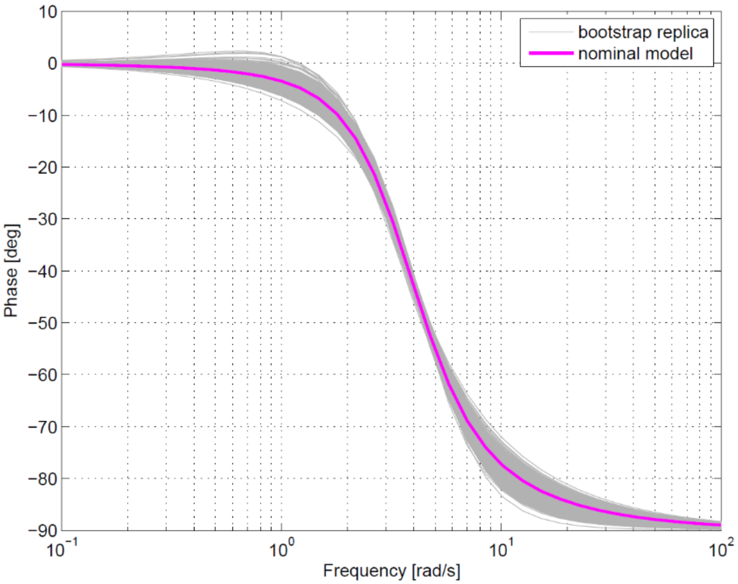

Bootstrap based approach applied on PI-MOESP model (1000 replications)

- ✓ On test-bed attitude pitch dynamics captured with very good accuracy (limited uncertainty band throughout considered freq. range)
- ✓ Thanks to higher test repeatability and pitch attitude dynamics decoupling w.r.t. longitudinal one assured by operating on test-bed in comparison with flight identification

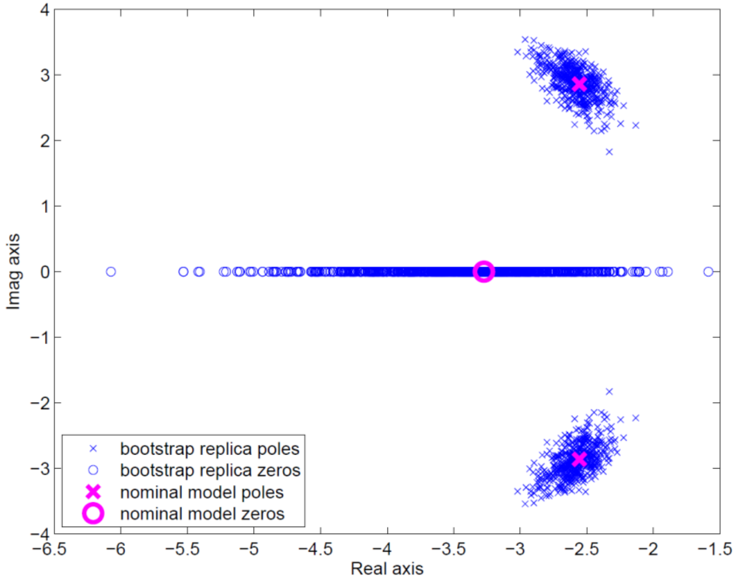

Additive uncertainty

$\mathcal{G} := \{G(s) = G_{NOM}(s) + W_{\Delta}(s)\Delta(s), \quad \|\Delta\|_{\infty} < h\}$

$\Delta(s)$: uncertainty LTI SISO random dynamics

$W_{\Delta}(s)$: stable, minimum phase, shaping filter, order 3

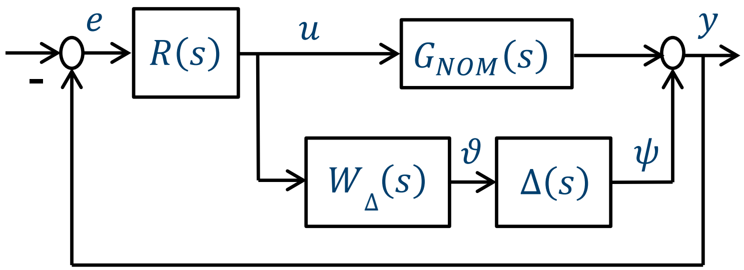

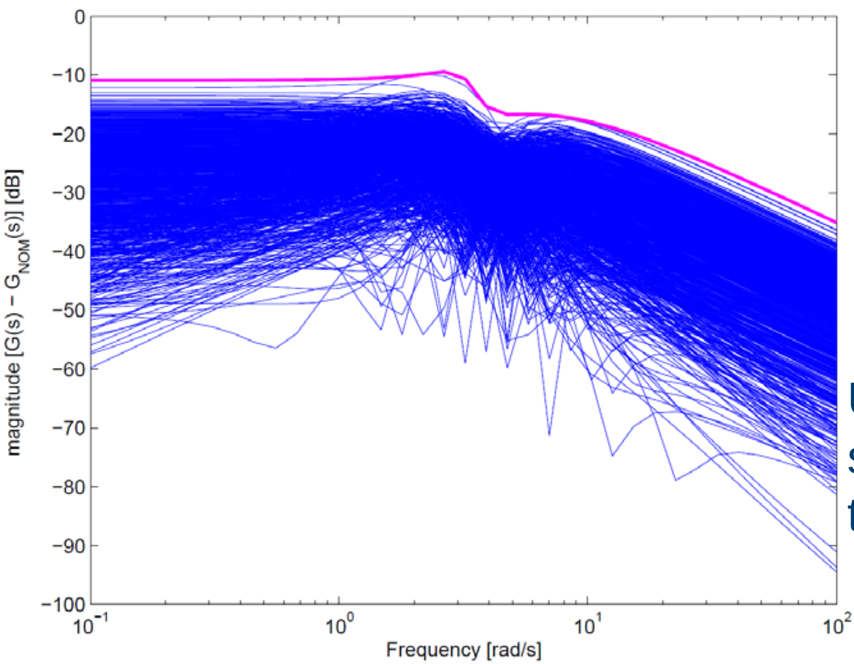

Robust stability limit

$h_{lim} = (\|W_{\Delta}(s)V_{NOM}(s)\|_{\infty})^{-1}$

- = 0.0880 for standard tuning
- = 0.0347 for optimal tuning

Uncertainty block peak gain equal to robust stability limit h_{lim} (worst case), randomly sampled to generate 1000 Monte Carlo simulations

Control design procedure test case
Monte Carlo simulation results (set-point tracking)

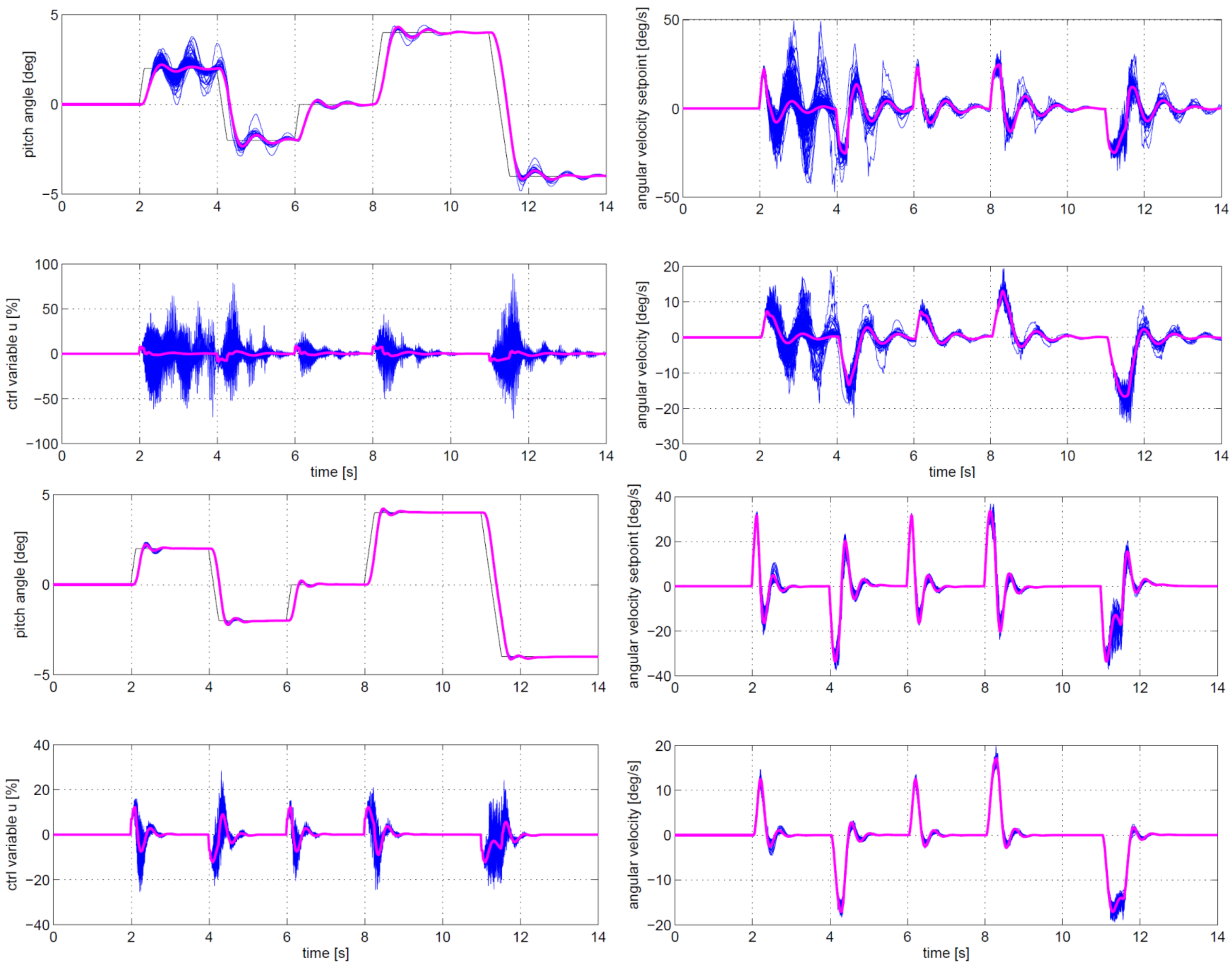

Magenta line: nominal model

Blue lines: uncertain models

Standard tuning

Optimal tuning

Control design procedure test case

Monte Carlo simulation results (load disturbance)

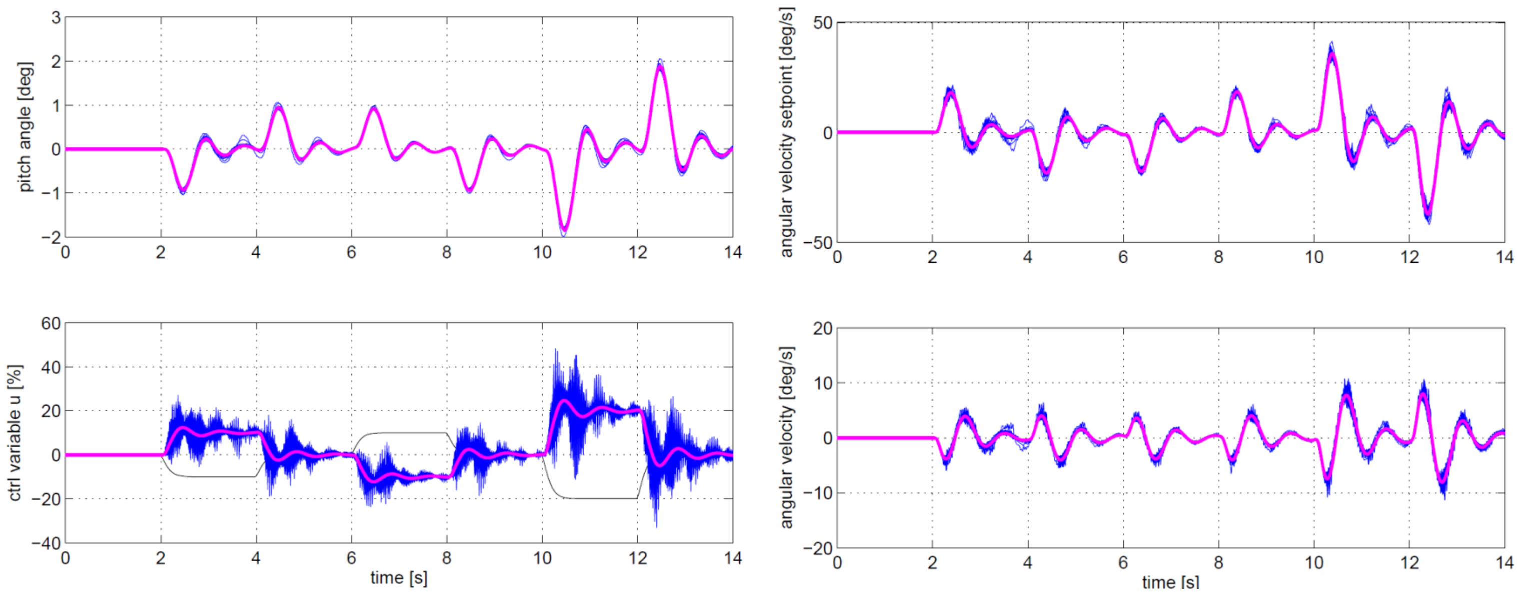

Standard tuning

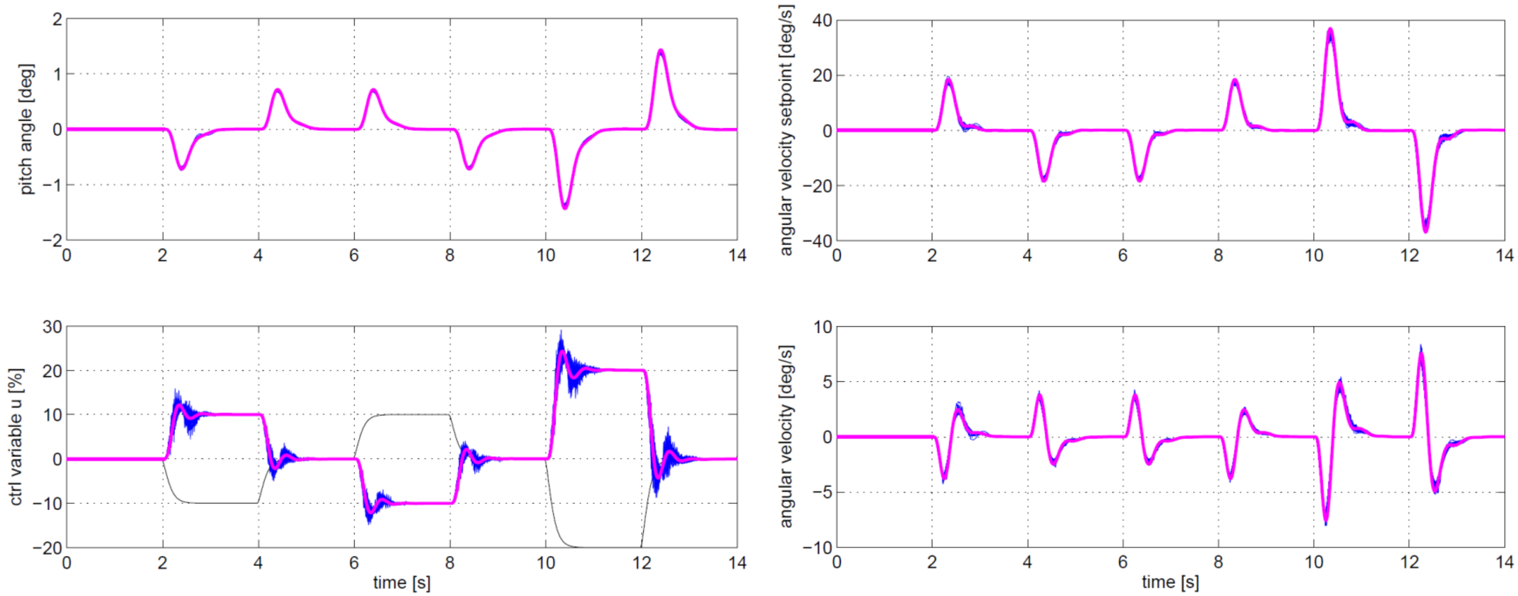

Optimal tuning

Control design procedure test case

Experimental results on test-bed (set-point tracking)

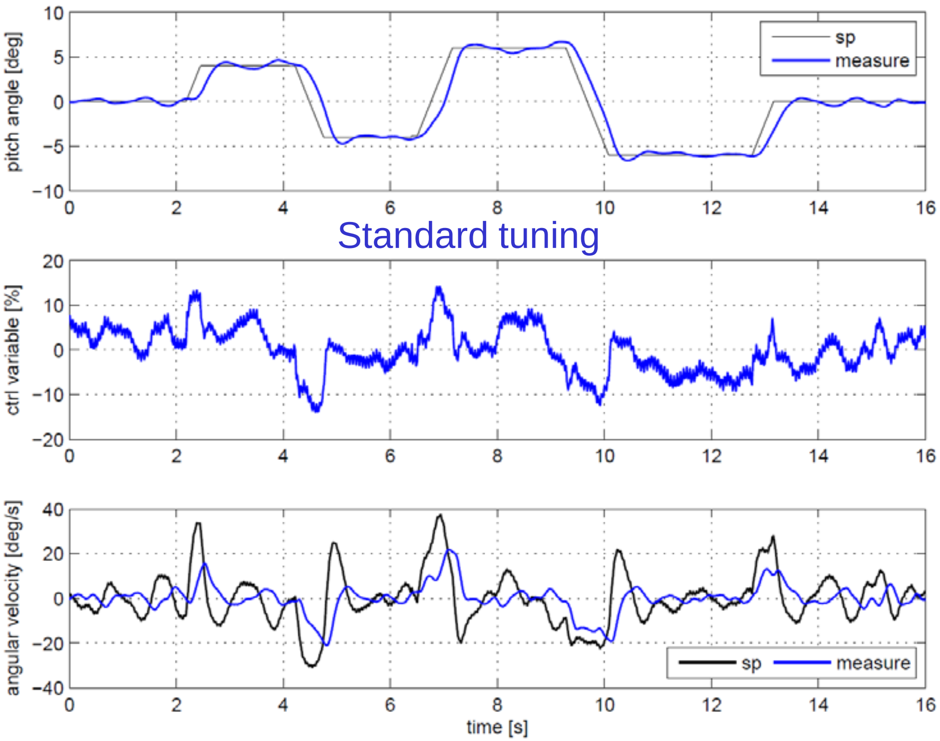

- Base throttle = 60% (hovering value)
- Angular sp variation requested
- Pitch control variable saturation = ±30%
- Rotors in OGE
- Aerodynamic disturbances due to rotors wake recirculation in closed indoor test area

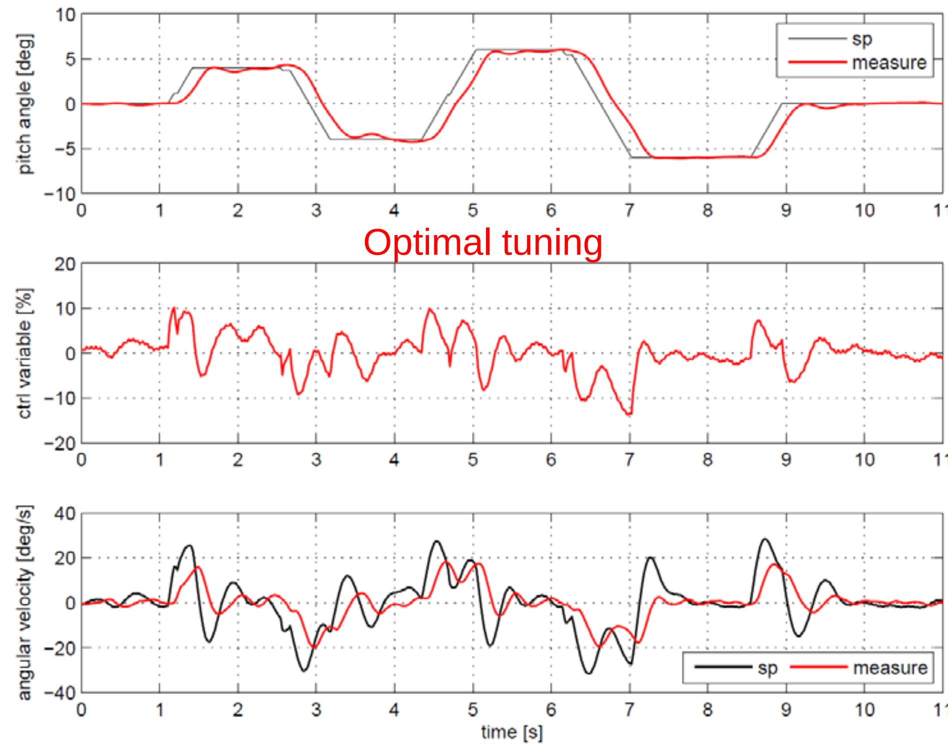

Opti tuning shows w.r.t. std one:

- ✓ reduced oscillations around angular sp
- ✓ remarkable amplitude lowering of the high frequency control variable oscillation
- ✓ smoothing of control action can be appreciate also on angular velocity

Control design procedure test case
Experimental results on test-bed (load disturbance)

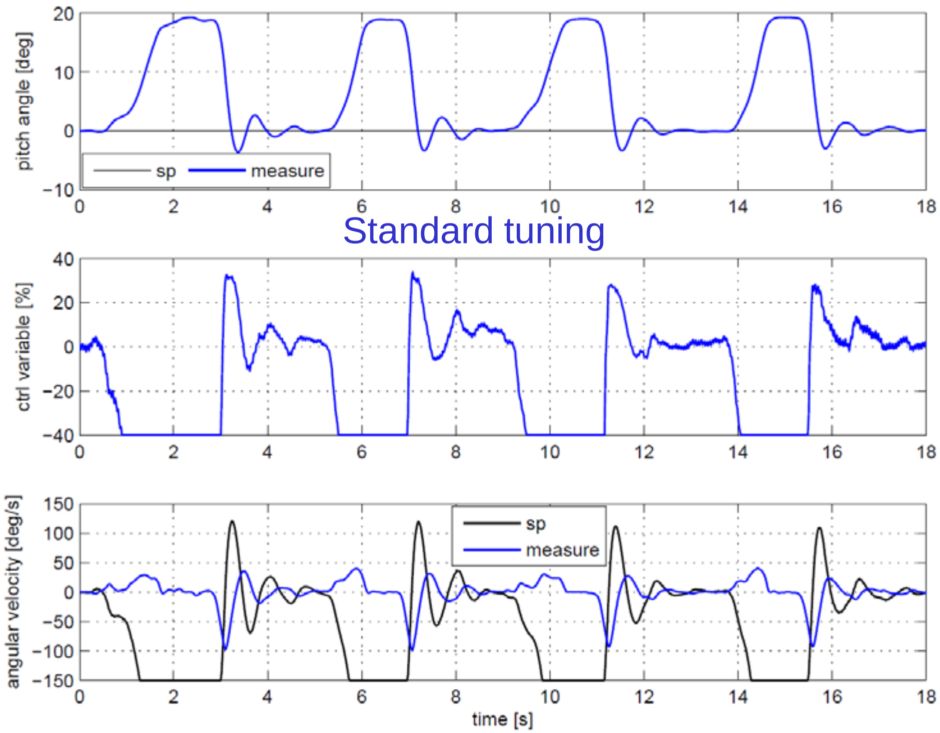

- To simulate the effect of an heavy wind gust, at the tip of the front arm was fixed a rope, pulled manually to impose a pitch angle of about 20°, maintained for a couple of sec. and hence suddenly released,
- Required null angular sp during the operation
- Pitch control variable saturation = ±40%
- Angular rate sp saturation = ±150°/s

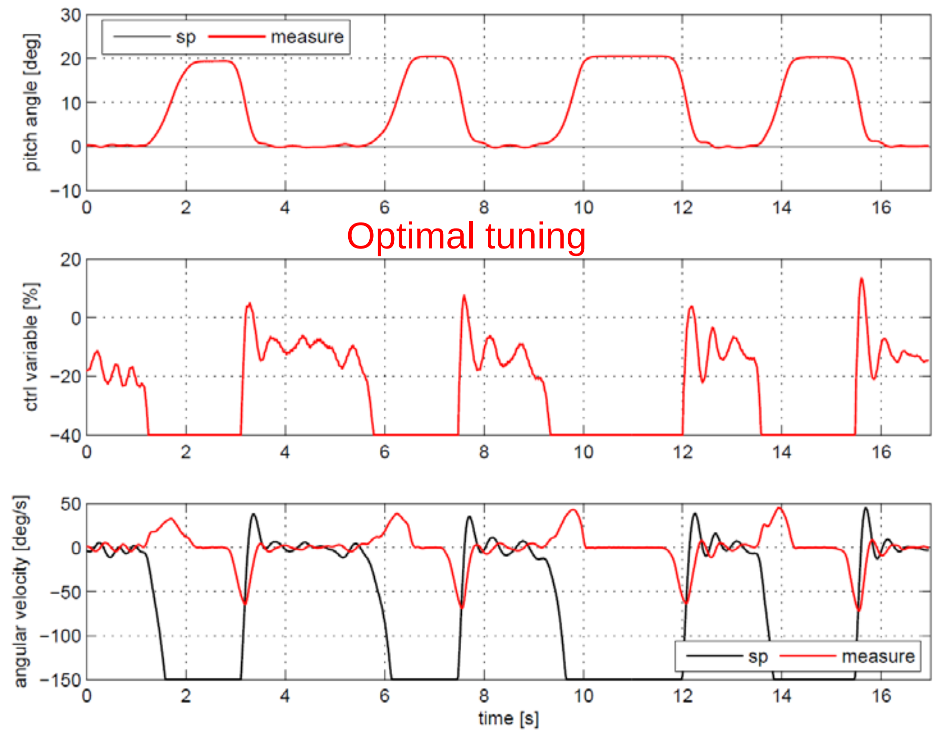

✓ pitch angle overshoot and oscillations in sp recovery occurring when imposed angular drift is released are eliminated adopting the optimal tuning

Control design procedure test case

Experimental results in flight (pitch axis)

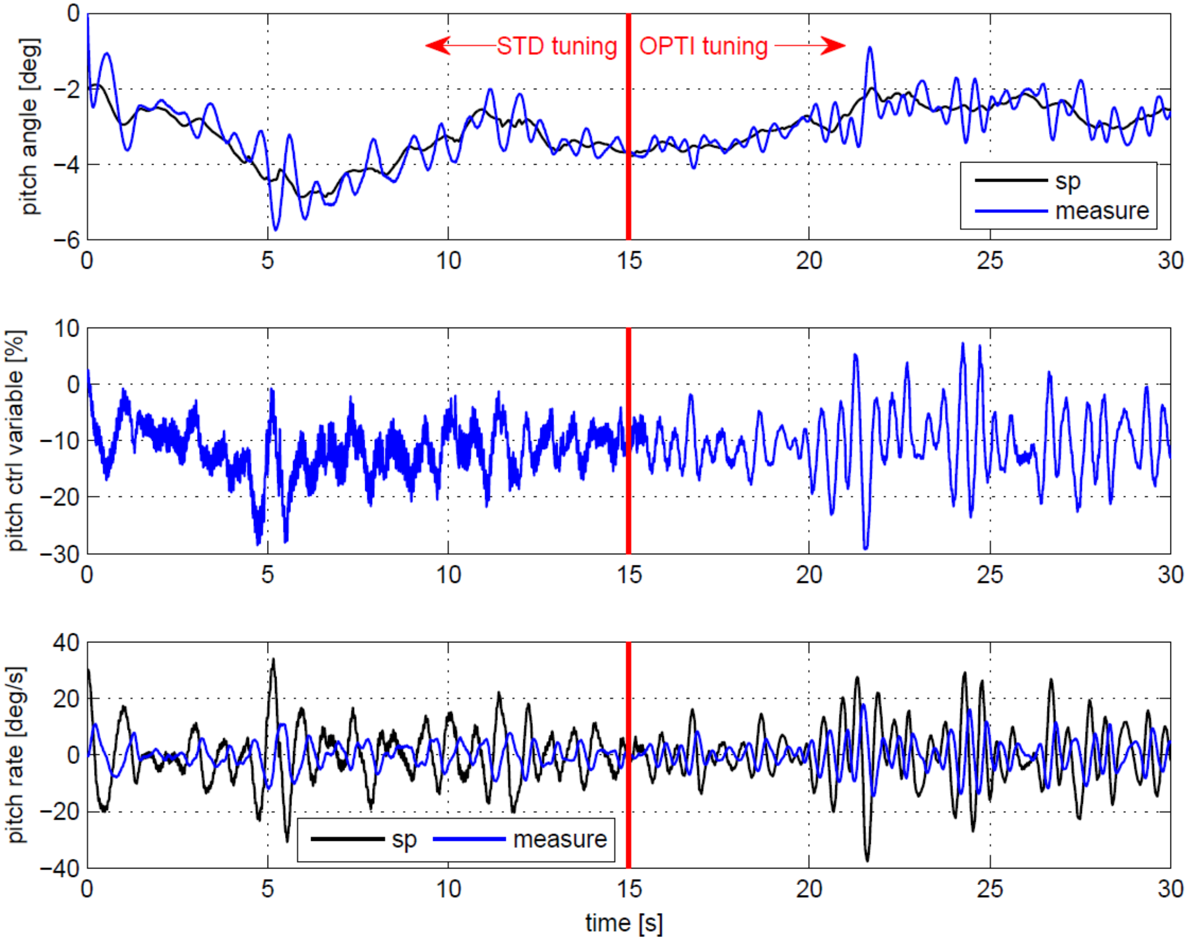

- Results logged during an OGE hovering at MTOW (height = 5m)
- Mean wind measured on ground of 2.5 m/s
- Position control is active, in the task of hold the desired x, y, z
- No pilot actions on commands
- Pitch (roll) angle sp requested to attitude controller is determined by longitudinal (lateral) position controller
- The switch from standard tuning to optimal one was commanded in flight

✓ The presence of wind disturbance determines a non-zero mean value of pitch angular sp to assure the position hold

✓ Switching to optimal tuning is evident a huge amplitude lowering of high frequency ctrl variable oscillation and as consequence a reduction of pitch angle oscillation amplitude around sp

Control design procedure test case
Experimental results in flight (roll axis)

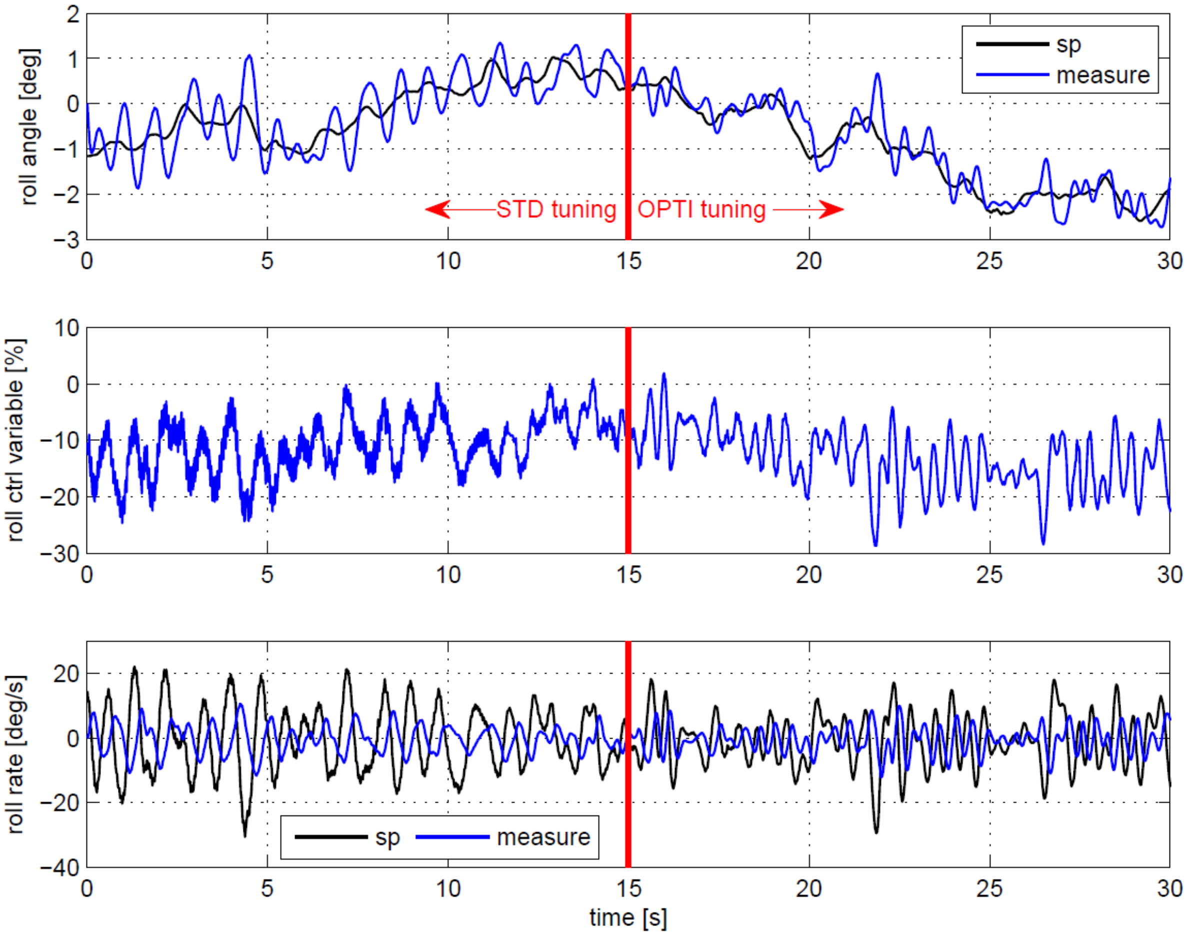

- Thanks to the geometrical and inertial symmetry of quadrotor the pitch controller tuning was applied also to roll
- The results correspond to the same flight portion considered in previous slide
- Analogous evidences can be observed

Concluding remarks

- The proposed integrated attitude control design procedure (from model identification to control synthesis), specifically addressed to near hovering condition, was developed and successfully applied to the considered quadrotor prototype pitch DoF

- Simulations demonstrate that structured H_∞ optimal tuning obtained with test-bed model in the loop can be applied also in flight with a non-significant loss in control performance, hence the attitude controller tuning can be achieved using models obtained in safe, faster and more repeatable identification experiments executed indoor

- In order to strengthen procedure validity, the entire tool chain was successfully applied to the production Aermatica quadrotor (with significant increment in size/weight w.r.t. prototype): flight test results confirm the expected simulation evidences

- In order to complete the tool chain the work will be naturally extended to yaw DoF

- As future work extension, a similar integrated procedure may be developed for the translational quadrotor DoFs

References

F. Riccardi
"Model identification and control of variable pitch quadrotor UAVs"
PhD thesis, Politecnico di Milano, 2015

F. Riccardi, M. Lovera
"Robust attitude control for a variable-pitch quadrotor"
IEEE 2014 Multi-conference on Systems and Control, 8-10 October, Nice, FR

P. Panizza, F. Riccardi, M. Lovera
"Black-box and grey-box identification of the attitude dynamics for a variable-pitch quadrotor"
ACNAAV 2015 – IFAC Workshop on Advanced Control and Navigation for Autonomous Aerospace Vehicles, June 10-12, Seville, ES

F. Riccardi, P. Panizza, M. Lovera
"Identification of the attitude dynamics for a variable-pitch quadrotor UAV"
40th European Rotorcraft Forum 2014, 2-5 September, Southampton, UK

QUESTIONS ?

marco.lovera@polimi.it